MISSILE & SPACE SYSTEMS DIVISION
DOUGLAS AIRCRAFT COMPANY, INC.
SANTA MONICA/CALIFORNIA

DOUGLAS

FEASIBILITY STUDY OF THE ULTRAVIOLET SPECTRAL ANALYSIS OF THE LUNAR SURFACE

By Norman N. Greenman, Valerie W. Burkig,
H. Gerald Gross, and J. Fred Young

Prepared under Contract No. NAS9-3152 by
Missile & Space Systems Division
Douglas Aircraft Company, Inc.
Santa Monica, California

for
Manned Spacecraft Center
National Aeronautics and Space Administration
Houston, Texas

Douglas Report SM-48529
March 1965

CONTENTS

FIGURES AND TABLES

FEASIBILITY STUDY OF THE ULTRAVIOLET SPECTRAL ANALYSIS OF THE LUNAR SURFACE

By Norman N. Greenman, Valerie W. Burkig,
H. Gerald Gross, and J. Fred Young
Douglas Aircraft Company, Inc.

SUMMARY

23705

The reflectance and luminescence characteristics in the 2000-3000 Å range of granite, gabbro, and serpentinite samples, in solid and granular form, have been studied for the purpose of determining whether it is feasible to map the surface composition of the moon by spectral analysis in this range from a manned lunar orbiting vehicle at 8 to 80 miles altitude. Luminescence was excited by ultraviolet radiation, x-rays, protons, and electrons.

Results of the experimental work show that (1) the reflectance declines gradually from 3000 Å to 2000 Å in a featureless curve for all samples and shows no consistent variation with grain size, (2) maximum reflectance is about 14%, minimum about 4%, with serpentinite showing a generally lower reflectance than granite and gabbro, which are about the same, (3) granite shows the greatest luminescence intensity, gabbro the next, and serpentinite the least in virtually all measurements, (4) luminescence intensity generally declines with decreasing grain size, but the spectral curve shape is not obscured, (5) except for sharp peaks at 3400 Å and 3600 Å, possibly due to element line emission, found with x-ray excitation in all samples, the luminescence spectra are broad band, but features such as peak positions and curve shapes (chiefly in wavelengths longer than 3000 Å) serve to distinguish rock types, (6) most of the luminescence is in the visible and near-ultraviolet wavelengths; only a small portion is in the 2000-3000 Å region, and (7) luminescence efficiencies in the 2000-3000 Å region are of the order of 1% for 1800-2200 Å ultraviolet excitation and of the order of 5×10^{-5}% for proton excitation. The latter is an upper limit for x-ray and electron excitation efficiencies, which are judged to be generally much less.

These laboratory results were combined with available knowledge of the space radiation environment of the moon to determine the feasibility of compositional mapping from a manned lunar orbiting vehicle. It is concluded that (1) on the sunlit side of the moon almost all the luminescence is due to ultraviolet excitation, it is intense enough to be detected, and it can be detected against the high reflected background by comparing the ratio of depth to continuum of a Fraunhofer line from the solar and lunar spectra, (2) on the dark side no background of 2000-3000 Å light is present, but the luminescence from x-rays, protons, and electrons is at or below the present detectability limits unless, as is possible, more energy is available from these sources than is estimated; in this case, the luminescence can be detected by directly viewing the lunar surface with a sensitive phototube, and (3) the compositional differences appearing in the experimental work are deemed detectable from the lunar orbiting vehicle and can be even more valuable when they are tied in with laboratory luminescence tests on rock samples returned from lunar landings.

INTRODUCTION

An understanding of the origin and history of the solar system is one of the primary scientific objectives of the nation's space program. Probably the first major step toward this objective will be achieved when the nature and composition of the lunar surface becomes known. In addition to its general scientific value, lunar compositional information is important for the establishment of lunar bases; decisions relating to base sites, building materials, and water availability will all be affected by the nature and composition of the moon's surface. Thus, for both scientific and practical reasons, the composition of large areas of the moon's surface should be mapped. Since the surface area of the moon is roughly one-fourth that of the land area of the earth, however, it is evident that the early manned Apollo landings, or for that matter, the unmanned soft landings that precede them, are not likely to supply all the information required. Valuable though they may be, they will provide only a few point samplings of the lunar surface.

The incorporation of a manned lunar orbiting vehicle into the Apollo program provides an excellent opportunity to obtain the required large-scale compositional mapping if a suitable analytical technique can be devised. This report presents the results of an eight-month study of the feasibility of one suggested technique--the analysis of the ultraviolet spectrum of the moon in the 2000-3000 Å region. The study was performed under contract NAS 9-3152 with the National Aeronautics and Space Administration, Manned Spacecraft Center, Houston, Texas, executed June 23, 1964, on the basis of Request for Proposal No. MSC 64-1176P, dated April 20, 1964. The purpose of the study is to determine whether the radiation characteristics of possible lunar surface materials in the 2000-3000 Å region are such as to allow compositional determinations to be made from a manned lunar orbiting vehicle at 8 to 80 miles altitude and, if so, what conditions must be met to accomplish that task.

The approach to the problem is four-fold. First, the types and intensities of radiation impinging on the moon — the space radiation environment — are delineated. Second, terrestrial rocks that may exist on the lunar surface are selected and their reflectance and luminescence characteristics in the 2000-3000 Å region are experimentally determined. Third, the characteristics of the radiation from the lunar surface in this wavelength interval are next calculated. Fourth, the results of this calculation are used to determine the conditions under which compositional mapping is feasible.

In carrying out this study, the authors were greatly assisted by W. B. Milton and T. H. Mills in the experimental phases of the work. R. E. Santina was most helpful in assembling the data on the space radiation environment of the moon, and N. H. Schroeder was also helpful in supplying information on problems of lunar orbiting vehicle instrumentation. A. J. Masley and J. A. Ryan provided excellent advice and suggestions throughout the course of the study.

SPACE RADIATION ENVIRONMENT OF THE MOON

The important sources of energy that may give rise to lunar radiation in the 2000-3000 Å region are ultraviolet radiation from the sun; x-rays from solar and cosmic sources; protons from the solar wind, solar cosmic ray events, and galactic cosmic rays; and electrons from the solar wind and galactic cosmic rays.

Ultraviolet Radiation

The solar ultraviolet energy distribution in the range of interest of this study is given by Hinteregger (1962) as follows:

Wavelength (Å)	Energy Flux at Moon
3000 - 2800	1×10^4 ergs/cm^2 sec
2800 - 2600	5×10^3 ergs/cm^2 sec
2600 - 2400	2×10^3 ergs/cm^2 sec
2400 - 2200	1.1×10^3 ergs/cm^2 sec
2200 - 2000	5×10^2 ergs/cm^2 sec
2000 - 1800	2×10^2 ergs/cm^2 sec
1800 - 1300	6×10^1 ergs/cm^2 sec

The fluxes at shorter wavelengths are very low.

X-Rays

The solar x-ray energy flux in the band from 8 Å to 100 Å is about 10 ergs/cm^2 sec at solar maximum (Friedman, 1960; Kreplin, 1961). At wavelengths less than 8 Å the energy flux is less than 0.6×10^{-3} erg/cm^2 sec. (Kreplin, Chubb, and Friedman, 1962). During solar cosmic ray events the solar x-ray flux increases about one order of magnitude (Chubb, Friedman, and Kreplin, 1960).

Cosmic x-rays, apparently galactic, have been measured as emanating from the vicinity of Scorpius, the Crab Nebula, and eight other sources (Bowyer et al., 1965). The total flux of these x-rays in the 1.5 - 8 Å band is 7×10^{-7} erg/cm^2 sec. This should be regarded as a lower limit because of the lack of data concerning wavelengths greater than 8 Å and also because other, as yet undetected, cosmic x-ray sources may exist.

The Solar Wind

As a result of the expansion of the solar corona, protons and electrons are accelerated to velocities of approximately 400-700 km/sec. With a spatial density of 1-10 ions/cm^3 at 1 A.U. the energy flux of the solar wind is in the range 3.2×10^7 - 1.75×10^9 keV/cm^2 sec, or 0.04 - 3 ergs/cm^2 sec. The energy flux of the solar wind is, therefore, much less than that of the solar ultraviolet. Solar wind energy flux may be further diminished if there is an appreciable lunar magnetic field. If such a field exists, however, it is possible, under some conditions, for solar wind particles to reach the dark side of the moon and significantly increase the energy flux from this source.

Magnetospheric Particle Radiation

Since the earth's magnetic field may extend past the lunar orbit (approximately 60 earth radii), (Ness, 1964), it is possible that energetic protons and electrons in the magnetosphere could reach the vicinity of the moon. If we assume a flux of 10 particles/cm^2 sec, and an average energy of 50 keV, the energy flux is ~ 0.02 erg/cm^2 sec. This energy density will not contribute significantly to sunlit side luminescence because of the dominant ultraviolet energy source. On the dark side, however, in the absence of ultraviolet, it could become an important energy source for luminescence production.

Solar Cosmic Rays

Protons incident on the moon during solar cosmic ray events could provide an important energy source, especially for the dark side. It may be possible for these particles to reach the dark side during the isotropic part of the events. Although it is very difficult to determine the energy deposited on the surface of the moon from these higher energy protons, we can make an estimate for the purposes of this study. We define the surface layer to be the top 1/10 gram/cm^2 of matter on the moon.

To estimate the total energy incident upon the lunar surface from a solar cosmic ray event, the flux and energy spectrum of the November 12, 1960, event is considered. The spectral distribution for that event may be written as follows (Ogilvie, Bryant, and Davis, 1962; Masley and Goedeke, 1963):

$$\phi = 3 \times 10^{12} \text{ p/cm}^2 \qquad \text{for } 0.2 < E < 0.35 \text{ MeV}$$

$$\phi = 0 \qquad 0.35 < E < 2 \text{ MeV}$$

$$\phi(>E) = 1.8 \times 10^{12} E^{-1.5} \qquad \text{for } 2 < E < 30 \text{ MeV}$$

$$\phi(>E) = 8.9 \times 10^{12} E^{-2} \qquad \text{for } 30 < E < 100 \text{ MeV}$$

(These values are based on experiments with rocket-borne detectors. The failure to detect particles with energies between 0.35 and 2 MeV may be due

to interactions with the geomagnetic field, so that this spectrum may not strictly represent that affecting the moon.)

The energy from this event that was deposited on the top 1/10 gram/cm^2 is on the order of 2 x 10^6 ergs/cm^2. If the event is assumed to have lasted 2 days, the energy deposition rate is approximately 10 ergs/cm^2 sec, almost all of which is from protons of energy less than 10 MeV.

It is unlikely that a solar cosmic ray event of this magnitude will occur during the time measurements are being made from the manned lunar orbiting vehicle; such an event occurs only about once a year at solar maximum. Smaller solar cosmic ray events (those that would deposit a dose of less than 100 rads behind 1 gm/cm^2 shielding) occur approximately once a month near solar maximum (1968-1970). Assuming that these events have the same spectral distribution as that of the November 12, 1960 event, the energy deposited on the lunar surface during solar cosmic ray events averages approximately 0.1 to 1 ergs/cm^2 sec.

Galactic Cosmic Rays

The energy deposited by galactic cosmic ray protons on the first 1/10 gram/cm^2 of the lunar surface is approximately 10^{-6} erg/cm^2 sec if a flux of 3 p/cm^2 sec is assumed. Galactic cosmic ray electrons deposit about 10^{-8} erg/cm^2 sec.

Table 1 summarizes the data on the space radiation environment of the moon.

LUNAR SURFACE MATERIALS

Composition

Direct knowledge is lacking of both the composition of the moon and the processes that operate upon it. Hence, the selection of terrestrial materials that approximate those of the moon is necessarily governed by the accepted theories of solar system origin and development, by analogy with terrestrial materials and processes, by knowledge of meteorites and tektites, and by astronomical observations and measurements, including the recent close range observations afforded by Ranger VII. None of these provide definitive information on composition and opinions differ widely. Urey (1952) postulates a composition similar to that of chondritic meteorite which approximates in composition the terrestrial ultra-basic rock peridotite. If the moon is homogeneous, its density suggests such a composition. On the basis of their recent observations of lunar luminescence in the Kepler region, Kopal and Rackham (1964) conclude that this area is composed of enstatite achondrites, which tends to confirm the meteorite aspect of Urey's hypothesis. This conclusion must be considered questionable, however, because in the laboratory studies upon which it is based only meteorite samples were used. Others, like Spurr (1945), consider the moon to have differentiated in a manner similar to the

TABLE 1

ENERGY FLUX TO LUNAR SURFACE
(ergs/cm^2 sec)

Source	Light Side	Dark Side	Comments
Ultraviolet Radiation			
From sun			
3000-2800 Å	1×10^4	0	
2800-2600 Å	5×10^3		
2600-2400 Å	2×10^3		
2400-2200 Å	1.1×10^3		
2200-2000 Å	5×10^2		
2000-1800 Å	2×10^2		
1800-1300 Å	6×10^1		
X-Rays			
From sun	10	0	Solar maximum, no flare activity
	100		Solar maximum, flare activity
From the galaxy	$\gtrsim 7 \times 10^{-7}$	$\gtrsim 7 \times 10^{-7}$	1.5 to 8 Å, thus, a lower limit; depends on moon-galaxy geometry
Protons			
Solar wind	$\lesssim 0.04$-3	$\lesssim 0.04$-3	If moon has a magnetic field, this flux may reach dark side.
Magnetospheric particles	$\lesssim 10^{-2}$	$\lesssim 10^{-2}$	
Solar cosmic rays	0.1-1	0.1-1	Must be performing experiment during solar cosmic ray event
Galactic cosmic rays	10^{-6}	10^{-6}	
Electrons			
Solar wind	$\lesssim 10^{-3}$	$\lesssim 10^{-3}$	If moon has a magnetic field this flux may not reach light side of moon, but may reach dark side.
Magnetospheric particles	$\lesssim 10^{-2}$	$\lesssim 10^{-2}$	
Galactic cosmic rays	10^{-8}	10^{-8}	

earth and to have produced granitic continents and basaltic maria. Baldwin (1963), though less definite about composition, visualizes the maria as being formed by volcanic flows, probably of basalt. O'Keefe and Cameron (1962), on the other hand, consider the maria to be made up of ash flows of granitic composition. On the basis of experiments with aerodynamic ablation of glass and observations of australites, Chapman and Larson (1963) conclude that this type of tektite, at least, has come from the moon. Tektite composition is chemically similar to granite; it is also similar to some types of terrestrial sandstones. Other hypotheses have been proposed, but, considering all the evidence, it is most reasonable to suppose that the lunar surface is composed largely of silicates. Based on the evidence of the earth and of the meteorites, these silicates are also probably igneous in nature. Meteorites are also probably present, but they average three parts ultra-basic igneous rock to one part iron. Their presence would only have the effect of diluting the igneous silicates with a moderate amount of iron.

The rock types for this study were therefore chosen from among the igneous rocks; three were chosen to represent, as well as possible, the entire range of the differentiation series. It would have been preferable to use mineral samples rather than rocks. Rocks, being aggregates of minerals, have a wider range of composition and can be expected to show a less uniform response than minerals. Therefore, the characteristics of any rock in the series can be calculated from the characteristics and known abundance of its constituent minerals. With the time and manpower conditions of the study, however, the rock samples are adequate. The compositions of the three rocks selected, determined from thin-section study, are as follows:

Granite. – (El Capitan formation, Mariposa County, California)

Quartz	10%
K-Feldspar	5
Plagioclase (An_{30})	60
Biotite	25

Accessories: green hornblende, titanite, apatite, zircon. Much of the plagioclase is zoned. The rock appears fresh with very little alteration.

Gabbro. – (Near San Marcos, San Diego County, California)

K-Feldspar	13%
Plagioclase (An_{45})	63
Biotite	15
Hornblende	3
Augite	6

Accessories: apatite, pyrite.
Much of the plagioclase is zoned. The hornblende commonly surrounds cores of augite and appears to have been derived from alteration of augite. Otherwise the rock appears fresh.

Serpentinite. – (Cape San Martin, Monterey County, California)

Serpentine	100%

The serpentine is in fine, fibrous, unoriented aggregates and in coarser, oriented, fibrous aggregates; some non-fibrous larger crystals are also present.

The granite and gabbro have been designated as such in the literature but do not represent the extremes of the acid-basic range. The granite has somewhat more plagioclase than is typical for that class, and the plagioclase of the gabbro is slightly more sodic than that of normal gabbro. The quartz content and plagioclase composition of the two, however, are such as to make them adequate representatives of acidic and basic types for the purposes of this study. The serpentinite was selected for two reasons; it is an ultra-basic representative and it contains water. This rock was considered a good candidate for the study because the ability to detect water-bearing lunar rocks is of prime importance in lunar exploration and some authorities believe that serpentinite, produced by hydration of olivine, may be present on the moon (Salisbury, 1961).

For all measurements except ultraviolet-excited luminescence, the rock samples were prepared by sawing slabs 1-1/2-inches square by 1/2-inch thick. These were lightly ground with carborundum paper to remove any saw marks. Smaller samples were prepared to fit the Tropel instrument for measurements of ultraviolet-excited luminescence. These were wafers 3/4-inch square and about 1/8-inch thick; they were given a high polish on one side with very fine carborundum polishing paper.

Grain Size

Previous studies have shown that serious degradation of the infra-red spectra of lithologic materials occurs as the grain size is decreased (Burns, 1963). Hence, in this study, measurements of several grain sizes of each rock type were made to see how this factor affected the ultraviolet spectra. Selection of appropriate grain size values was made difficult by uncertainty as to the state of aggregation of the lunar surface materials. It is generally agreed, on the basis of the measured thermal characteristics of the moon, that no significant amount of solid rock can be exposed at the surface. Most American and many European investigators believe that the lunar surface layer is composed of granular material; estimates of grain size, however, vary from approximately one micron to several hundred microns and actual grain size could even exceed this. The Ranger VII photographs added no information on this point except to show that no rubble was evident in the impact area. Sytinskaya (1959) has proposed a lunar surface of meteor slag. This highly vesicular material, with a porosity possibly exceeding 90%, is considered to be formed by the cooling in vacuum of molten material produced primarily during meteorite impact. Although this hypothesis is favored by some, no attempt was made in this study to assess the effects of such a surface.

To encompass the suggested size range as closely as practicable, a sand size and two powders were prepared from each rock type. One of the sets of powders was prepared by C. C. Mason at the Manned Spacecraft Center from rock samples supplied by Douglas. It was ground in a tungsten carbide ball mill, and the granite and gabbro powders were analyzed by the pipette method. The size data, supplied by Mason, are shown in figure 1. The serpentinite powder, though not analyzed, appeared to be similar to the other two. These are designated as the 8 micron samples in the report to follow. The remaining two sets were prepared at Douglas by crushing in a hardened steel mortar and pestle and grinding with procelain and alumina mortars and pestles. About 320 to 330 grams of each rock were ground to pass a 590 micron sieve. Some 50 to 60 grams were then split off from each of the ground portions and were further ground to pass a 44 micron sieve. These are designated the 590 micron and 44 micron samples, respectively, in the report to follow. Sieve analyses were made of the 590 micron samples; the resulting size data are shown in figure 1. No size analyses were made of the 44 micron samples but, by visual comparison with the 8 micron samples, they were found to be slightly coarser - no more than one, and probably closer to one-half, Wentworth grade. Their medians are therefore estimated as being between 11 and 16 microns.

The powders were moderately tamped down in their holders to prevent slumping and spilling during the measurements. They simulate, therefore, lunar grain sizes but not lunar porosities which are thought to be very high.

EXPERIMENTAL RESULTS

Ultraviolet Reflectance

Experimental techniques.— Two instruments were used for making reflectance measurements; a Cary Model 14 recording spectrophotometer and a Tropel Model N-1 monochromator and reflectometer. In the Cary 14, the light is normally incident on the sample and the reflected light is collected by an integrating sphere. By selected positioning of the sample, it is possible to detect the total reflected component, specular plus diffuse, or to eliminate the specular and record only the diffuse component. The incident monochromatic light illuminates the sample and a standard alternately and the electronically calculated ratio of the two reflected signals is presented on a chart as the spectrum is swept. The arrangement is shown in figure 2.

Magnesium carbonate was used as a standard in measuring the rock samples. It was subsequently run against magnesium oxide, for which absolute values of reflectance are given by Middleton and Sanders (1951), in order to calculate absolute values for the samples. The measurements of magnesium oxide given in the literature were carried only down to 2400 Å, but the variation in reflectance over wide ranges of the spectrum was so small that even with extrapolation to 2000 Å a constant value of 94.5% could be taken as representing the range 2000 to 3000 Å. With this value, the reflectance curve of the magnesium carbonate standard began with 93% reflectance at 3000 Å, continued essentially linearly to 84% at 2200 Å, and then declined progressively more steeply to about 73-1/2% at 2000 Å.

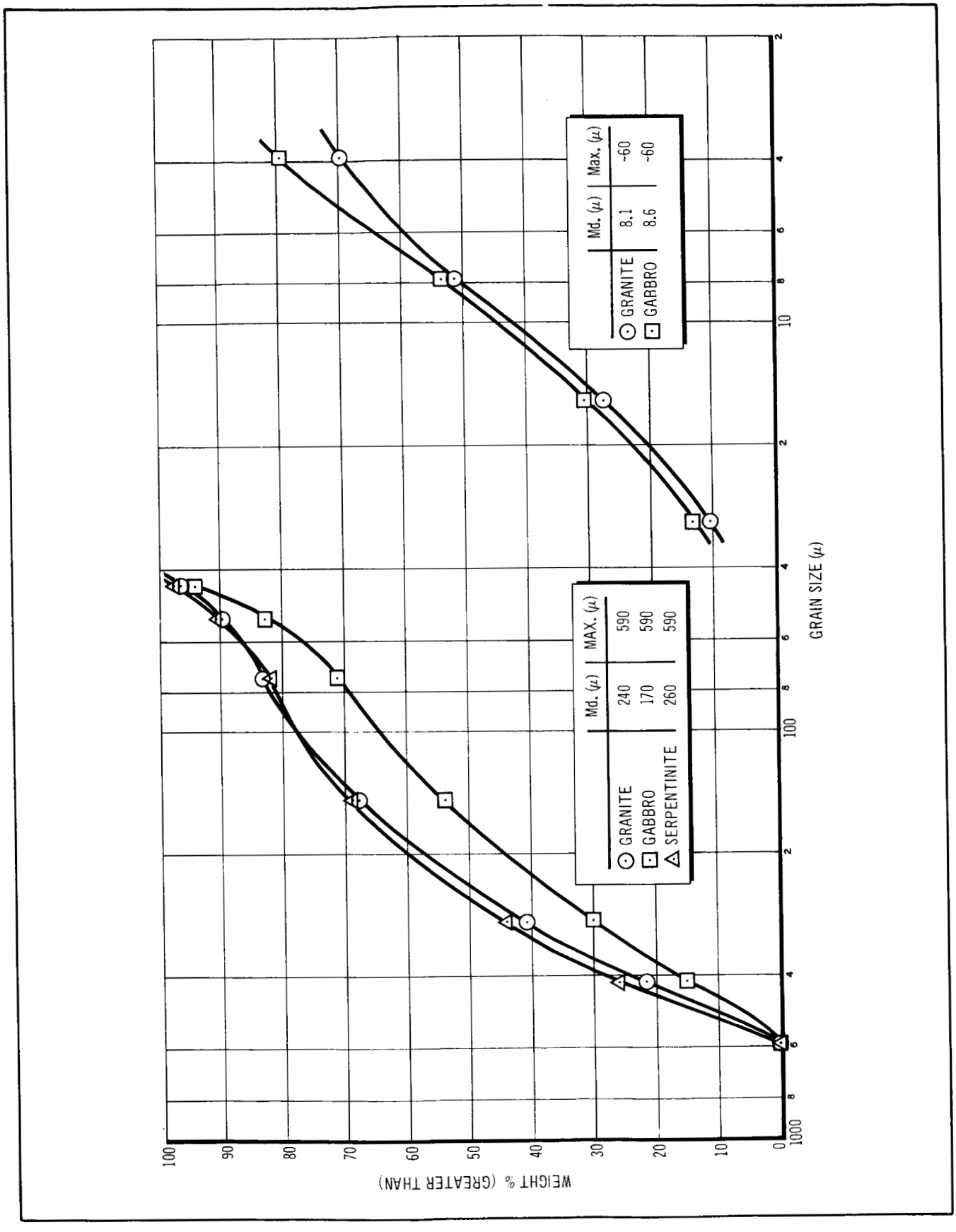

Figure 1 Grain Size Distribution −590μ and 8μ Samples
(8μ Sample Data From C.C. Mason, MSC)

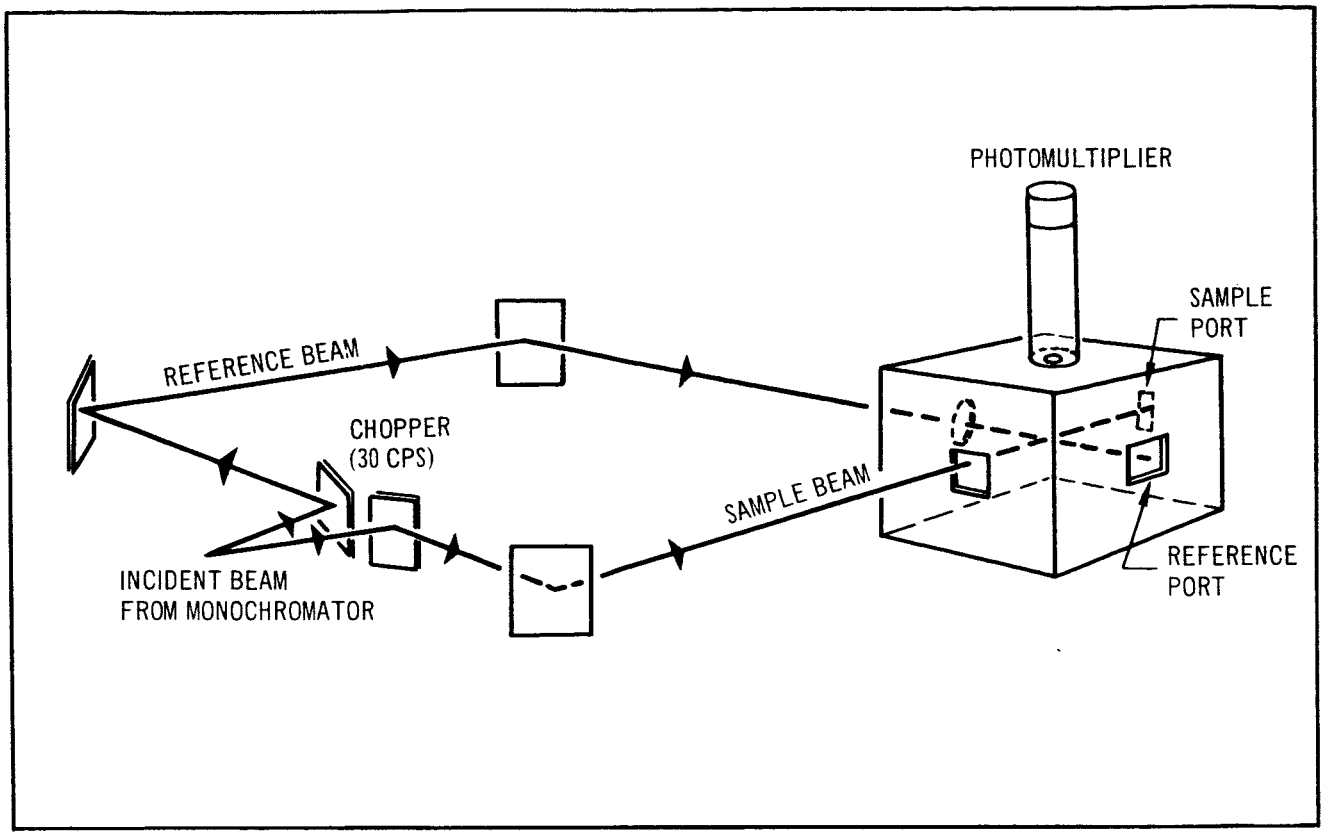

Figure 2 Reflectance Measurement System – Cary Model 14 Recording Spectrophotometer

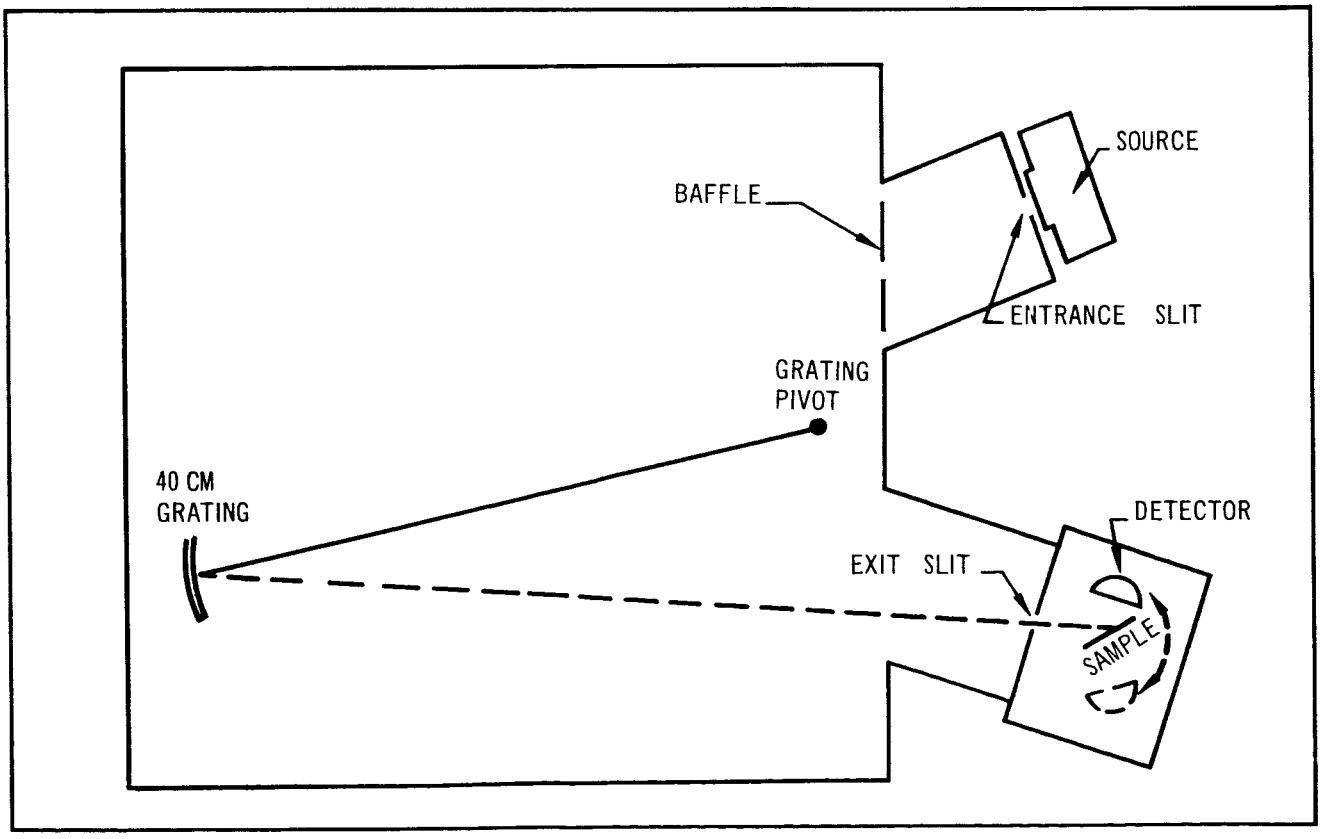

Figure 3 Tropel Monochromator Measurement System

By means of the integrating sphere,the Cary makes use of the largest possible signal. This, together with the continuously calculated ratio to the reflectance of a standard, leads to a greater accuracy than the Tropel can offer. However, it is not possible with the Cary to study the effects of varying angles of incidence and observation, while the Tropel is ideally suited to such measurements.

As shown in figure 3, the Tropel instrument consists of a 40 cm concave grating monochromator with a reflectometer mounted at the exit slit. A sample is mounted vertically in the reflectometer in the path of the emergent beam and can be rotated about a vertical axis to vary the angle of incidence, or can be raised out of the path of the beam when a measurement of the incident light is to be made.

Both the Cary and Tropel instruments require the illuminated surface of the sample to be vertical. To prevent the spilling of the granular samples, a quartz cover plate of about 1/2 mm thickness was used for the Cary measurements to hold the powder in the container. The small effect of the quartz was compensated by using an identical cover plate on the magnesium carbonate comparison standard and by measuring the reflectance of the quartz with no sample. For Tropel measurements, it was found that the 8 micron and 44 micron powders cohered so well when pressed firmly into small flat cups that they could be mounted vertically and used without a cover plate. The 590 micron grains required a quartz cover plate. The reflectance of the quartz, measured without sample, was then subtracted from the sample plus quartz measurements. This led to a large uncertainty in the result near the quartz specular peak but at other angles the quartz reflectance was negligible.

The detector in the Tropel, a sodium salicylate-coated glass light pipe leading to an EMI 9502S photomultiplier tube, can be rotated in a horizontal plane around the sample to vary the angle of observation or to detect the incident beam when the sample is withdrawn. Photons below 3000 Å are converted with nearly 100% efficiency in the sodium salicylate (Allison, Burns, and Tuzzolino, 1964) to photons of about 4400 Å which pass with little attenuation through glass and are near the peak of the phototube response. The detector response, therefore, is essentially flat in the 2000-3000 Å region.

For most of the experiment, the exit slit was kept at 250 microns to pass a 10 Å band of light. To better define the angle of observation, the 1/2 inch wide light pipe was covered except for a central 3/8 inch high by 1/8 inch wide area. This area received all of the incident beam and more than 80% of the specularly reflected beam from a polished sample, but only about 3% of the diffuse reflected light. Unlike the Cary, the Tropel has no means of continuous comparison with a standard or with the incident light. To avoid errors due to light source fluctuations, the reflected and incident intensities were measured consecutively at each wavelength point and the ratio was calculated. Source intensity variations and the small solid angle of detection limit the accuracy of the Tropel measurements, particularly for powdered samples. Therefore, the reflectance values given by the Cary are used in the calculations. Variations with angles of incidence and observation are qualitatively as indicated by the Tropel.

Calibration.— For comparison of the laboratory situation with that expected at the lunar surface, a calibration of the Tropel was required. The source used for this wavelength region was a tungsten filament in a tube with a quartz window. A calibration by the Bureau of Standards gives filament temperature vs applied voltage to a maximum of about 2500°K. This temperature gave some light down to 2400 Å but the shorter wavelength values are questionable. Since the intensity in the visible is several orders of magnitude higher, large scattered light signals from longer wavelengths were superimposed on the desired reading and it was found necessary to mount a Corning 7-54 filter at the entrance slit to cut out wavelengths above 4000 A.

From the filament temperature and the Planck function, the power per unit area emitted by the filament was calculated. Then from the geometry of the entrance slit, baffle dimensions, and spacing, the area of the filament seen by the grating was determined. This area was treated as a point source and the fraction of emitted light incident on the monochromator was calculated; this intensity vs wavelength was then corrected for the 7-54 filter transmission. The calculations are summarized in table 2 with the fourth column showing the intensity vs wavelength incident on 1 cm^2 at the entrance slit. The fifth column gives the output of the EMI tube in μA and the last column lists the calibration factor vs wavelength, combining the effects of the grating, photomultiplier, and geometry. With this calibration it is possible to estimate the signal from reflectance and from luminescence which the Tropel would give if it were on the lunar orbiting vehicle. Although some improvement may be obtainable with another instrument, it is of value to discuss the available light in terms of an instrument for which we have a calibration.

It appears that the factor is nearly a constant of about 3.2×10^{-3} erg/cm^2 sec Å incident on the instrument for an output signal of 1 μA. A constant factor is not unexpected because the geometry does not vary with wavelength and because over this range the grating should show little decrease of reflectance with wavelength. The use of sodium salicylate, as explained above, makes the phototube response flat in the 2000-3000 Å region.

Description of results.— The reflectance vs wavelength curves measured with both the Cary and Tropel show a gradual increase of reflectance with wavelength from 2000-3000 Å for all three rocks. No reflectance peaks were found in any case.

The reflectance coefficients vary from about 3% at 2000 Å for serpentinite to 14% at 3000 Å for gabbro. The difference between the granite and gabbro coefficients is slight, but the serpentinite values are significantly lower.

When the diffuse reflectance of different grain sizes is measured, however, the distinction between reflectance of different rock types is less clear. Table 3 summarizes the results.

TABLE 2

CALIBRATION OF TROPEL MONOCHROMATOR

Wavelength (cm)	Filament Emission (ergs/cm^2 sec Å)	7-54 Filter Transmission	Energy Flux into Tropel (ergs/cm^2 sec Å)	Phototube Output Per Å (μA)	Calibration Factor (ergs/cm^2 sec Å μA)
2.4×10^{-5}	2.00	0.15	0.39×10^{-4}	0.019	2.0×10^{-3}
2.5×10^{-5}	4.24	0.40	2.20×10^{-4}	0.057	3.9×10^{-3}
2.6×10^{-5}	8.44	0.57	6.25×10^{-4}	0.228	2.7×10^{-3}
2.7×10^{-5}	15.76	0.69	14.13×10^{-4}	0.437	3.2×10^{-3}
2.8×10^{-5}	28.09	0.78	28.45×10^{-4}	0.855	3.3×10^{-3}
2.9×10^{-5}	47.66	0.83	51.48×10^{-4}	1.52	3.4×10^{-3}
3.0×10^{-5}	77.70	0.86	86.80×10^{-4}	2.43	3.6×10^{-3}
					Average: 3.2×10^{-3}

i.e. 3.2×10^{-3} ergs/cm^2 sec Å incident on the Tropel entrance slit gives 1 μA from the EMI tube

For this calculation:

Filament emission, $E_{b\lambda}^{d\lambda} = \frac{3.697 \times 10^{-5}}{\lambda^5} \left(e^{\frac{1.432}{\lambda T}} - 1 \right)^{-1} d\lambda$, with wavelength, λ, in cm, T in °K (Planck's law)

T = 2500°K

Combined geometrical factor, $G = 1.30 \times 10^{-4}$

TABLE 3

DIFFUSE REFLECTANCE (%)

Grain Size	2000 Å		2500 Å		3000 Å	
	Cary	Tropel	Cary	Tropel	Cary	Tropel
Granite						
Solid	8	-	9-1/2	-	13-1/2	-
590μ	6-1/2	4	6-1/2	5-1/2	10	7
44μ	5-1/2	5-1/2	6-1/2	5-1/2	10	8-1/2
8μ	6	6-1/2	8	11	12-1/2	16
Gabbro						
Solid	9	-	9-1/2	-	14	-
590μ	7-1/2	7	8	10	12-1/2	15
44μ	8	4-1/2	8-1/2	9	13	17
8μ	7-1/2	11	9-1/2	10-1/2	15	13
Serpentinite						
Solid	3-1/2	-	4	-	5	-
590μ	5-1/2	3	4-1/2	2	5	4-1/2
44μ	6	4	7	5-1/2	15	8-1/2
8μ	5	4	5-1/2	5-1/2	12-1/2	10

For granite and gabbro, the polished samples gave higher total reflection than the granular samples but no clear distinction can be made between the grain sizes based on reflection coefficients. For serpentinite, the reflection from the granular samples was greater than from the polished samples with maximum coefficients found at 44μ.

The Tropel probe is estimated to pick up 3% of the diffuse reflectance so that multiplying the measured values by 33 allows a corresponding table to be made up from Tropel measurements of powdered samples. Values measured at 10° angle of incidence and 45° angle of observation were used. Due to the low signals, the uncertainty in readings is large and therefore the Cary values are probably more accurate. The comparison does show general agreement between the two instruments, but no clear distinction between rock types is evident from reflectance characteristics.

Figure 4 shows diffuse reflectance at 2000 Å for 8 μ granite for angles of incidence of 0°, 20°, 50°, and 70°. These are typical of the results found with all the powdered samples.

Within the accuracy of the measurement, no significant departure from uniform diffuse reflection was found as the detector was rotated around the sample. The intensity was not found to vary with the angle of incidence except that at large angles of observation an increase in intensity was noted. This specular reflection at grazing incidence for diffuse samples is predicted by theory.

For the polished samples, the shape and size of the specular peak was investigated as a function of angle of incidence over the 2000-3000 Å range. Figure 5 shows the reflected peak for angles of incidence of 20°, 50° and 70° for 2000 Å incident on polished granite.

These results are typical of those found at all wavelengths and with the other polished samples. The width at half-maximum is about 10° for each angle of incidence. The per cent reflection is seen to increase with angle of incidence, in agreement with the electromagnetic theory treatment of dielectric reflection. The amount of reflection at a particular angle of incidence depends upon the index of refraction of the material, but rises to 100% reflection at grazing incidence for all dielectric materials.

In order to investigate the effect of source intensity, two different hydrogen discharge tubes were used; the Hanovia lamp and the Nester lamp, the former having about twice the intensity of the latter. As was expected, no difference in reflection coefficient was detected. However, the ultraviolet at the lunar surface is about four orders of magnitude greater than that of our sources and could conceivably produce effects not detected in the laboratory.

Summary of ultraviolet reflectance.—For powdered samples, gabbro has the highest reflectance coefficients while granite and serpentinite are nearly the same and slightly lower than gabbro. No peaks are found in the reflectance curves, only a gradual rise with increasing wavelength.

	Average (2000-2500 Å)	Average (2500-3000 Å)
Gabbro	8%	11%
Granite	6-1/2%	9%
Serpentinite	5-1/2%	9%

No clear distinction can be made between grain sizes.

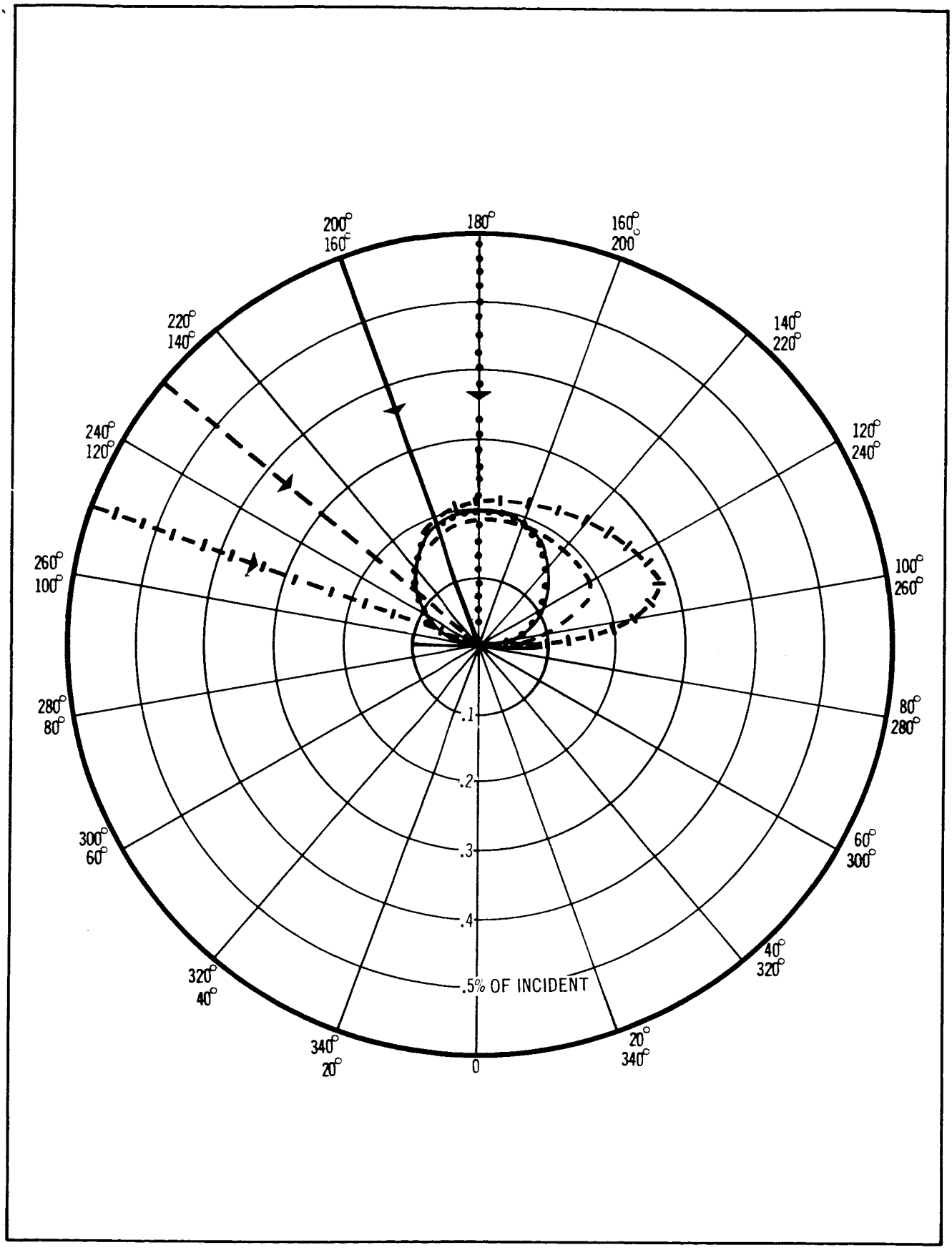

Figure 4 Diffuse Reflection vs Detection Angle for 0°, 20°, 50°, 70° Angles of Incidence (8 μ Granite, 2000Å)

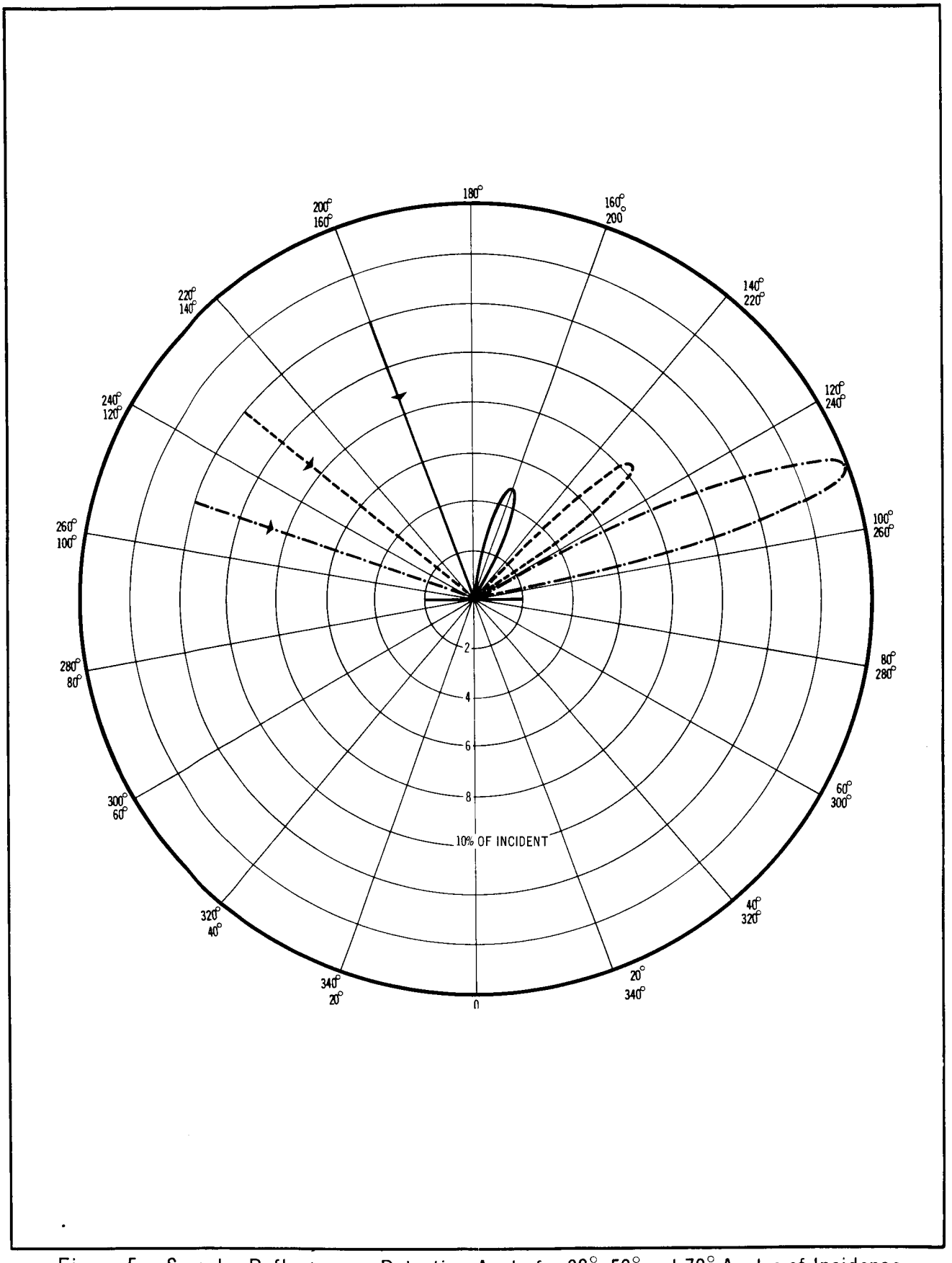

Figure 5 Specular Reflection vs Detection Angle for 20°, 50° and 70° Angles of Incidence (Polished Granite, 2000Å)

Ultraviolet-Excited Luminescence

Since the amount of energy incident upon the lunar surface from the ultraviolet region of the solar spectrum is orders of magnitude greater than that from particle bombardment, the luminescence excited by the ultraviolet is expected to be of great significance.

The samples were first placed at the entrance slit and illuminated by a hydrogen discharge tube so that the reflected light and luminescence entered the monochromator. However, because of the small solid angle subtended by the grating at the sample, the specular peak could barely be detected; diffuse reflection and luminescence could not be detected at all.

The samples were then placed in the reflectometer at the exit slit. They were illuminated by a small wavelength band, and the reflected and luminescent light was observed through filters. The advantage of this arrangement is that it is possible to see which incident wavelengths are responsible for producing luminescence, information not obtainable when all wavelengths are present simultaneously. The polished samples were mounted at about 60° to the incident beam so that the specularly reflected peak missed the detector probe which was set at 90° to the beam. The same arrangement was used for the powdered samples. The detected light, if present, was made up of diffuse reflection plus luminescence.

The filters used were three Corning filters and a piece of pyrex. Their transmission curves, shown in figures 6, 7, 8 and 9, were measured with both the Tropel and the Cary; they are in excellent agreement with those supplied by Corning. The significant characteristics of the filter curves are as follows:

(1) All four filters are nearly opaque at wavelengths shorter than 2200 Å.
(2) Pyrex is nearly opaque for wavelengths shorter than 3000 Å.
(3) The 9-54 transmission is significantly greater than that of the 9-30 in the 2200-2500 Å region.
(4) The 7-54 is nearly opaque at wavelengths longer than 4000 Å, whereas the other three filters transmit about 90% at these wavelengths.

Therefore, with appropriate combinations of incident wavelength and filter cutoffs, the reflected and luminescent components can be separated since the reflected component is at the same wavelength as the incident beam, whereas the luminescent component is at a longer wavelength (lower photon energy).

The filters, in a specially constructed mount, were inserted, each in turn, in front of the detector. The ratios of "filter in" to "filter out" measurements were then plotted and compared with the filter transmission curves. If the diffuse reflected component is designated by D, the luminescent component by L, and the respective filter transmission values by t_D and t_L, then the filter ratio

$$\frac{\text{"filter in"}}{\text{"filter out"}} = \frac{D\,t_D + L\,t_L}{D + L}$$

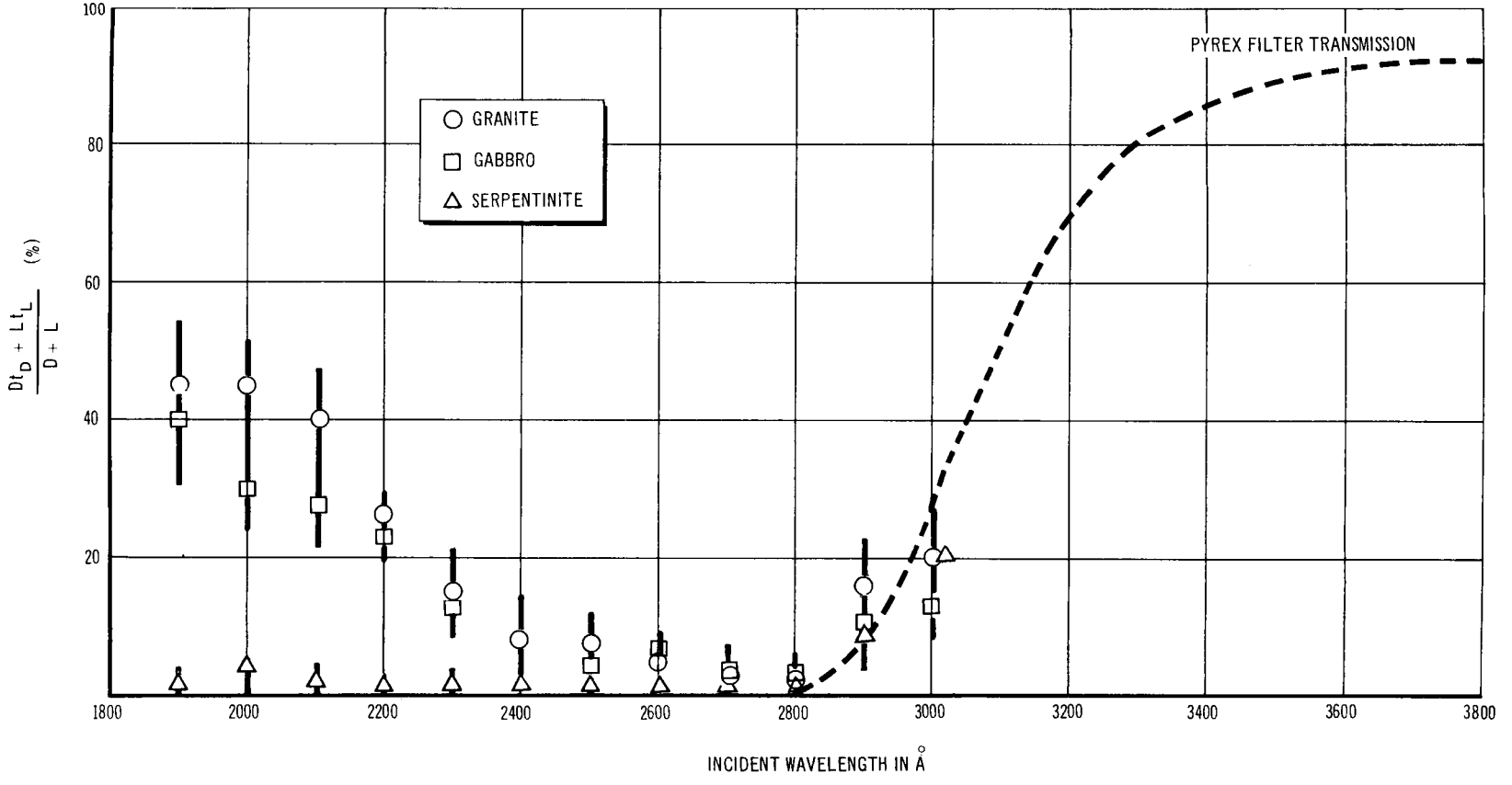

Figure 6 Transmission of Diffuse Reflection Plus Luminescence Through Pyrex Filter

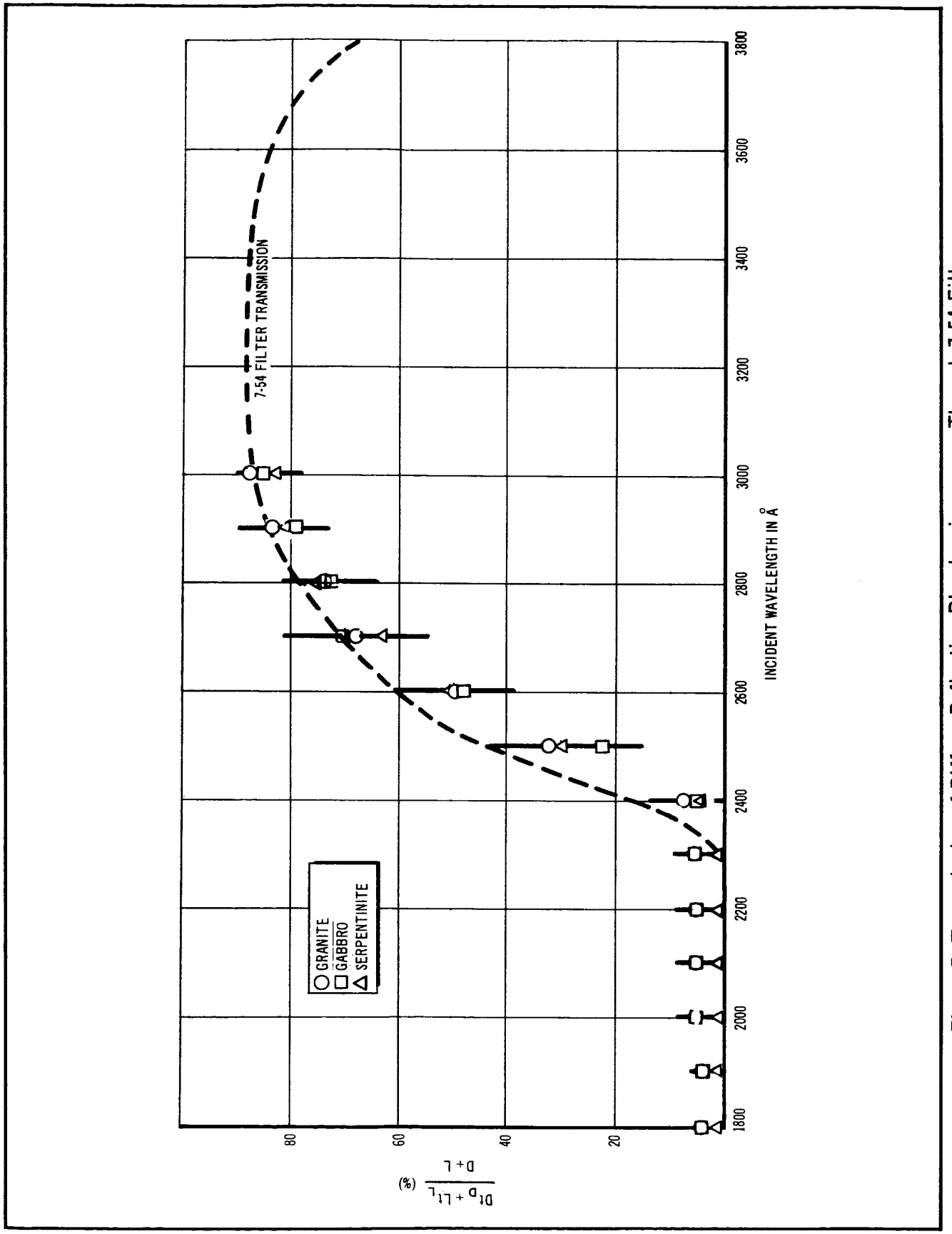

Figure 7 Transmission of Diffuse Reflection Plus Luminescence Through 7-54 Filter

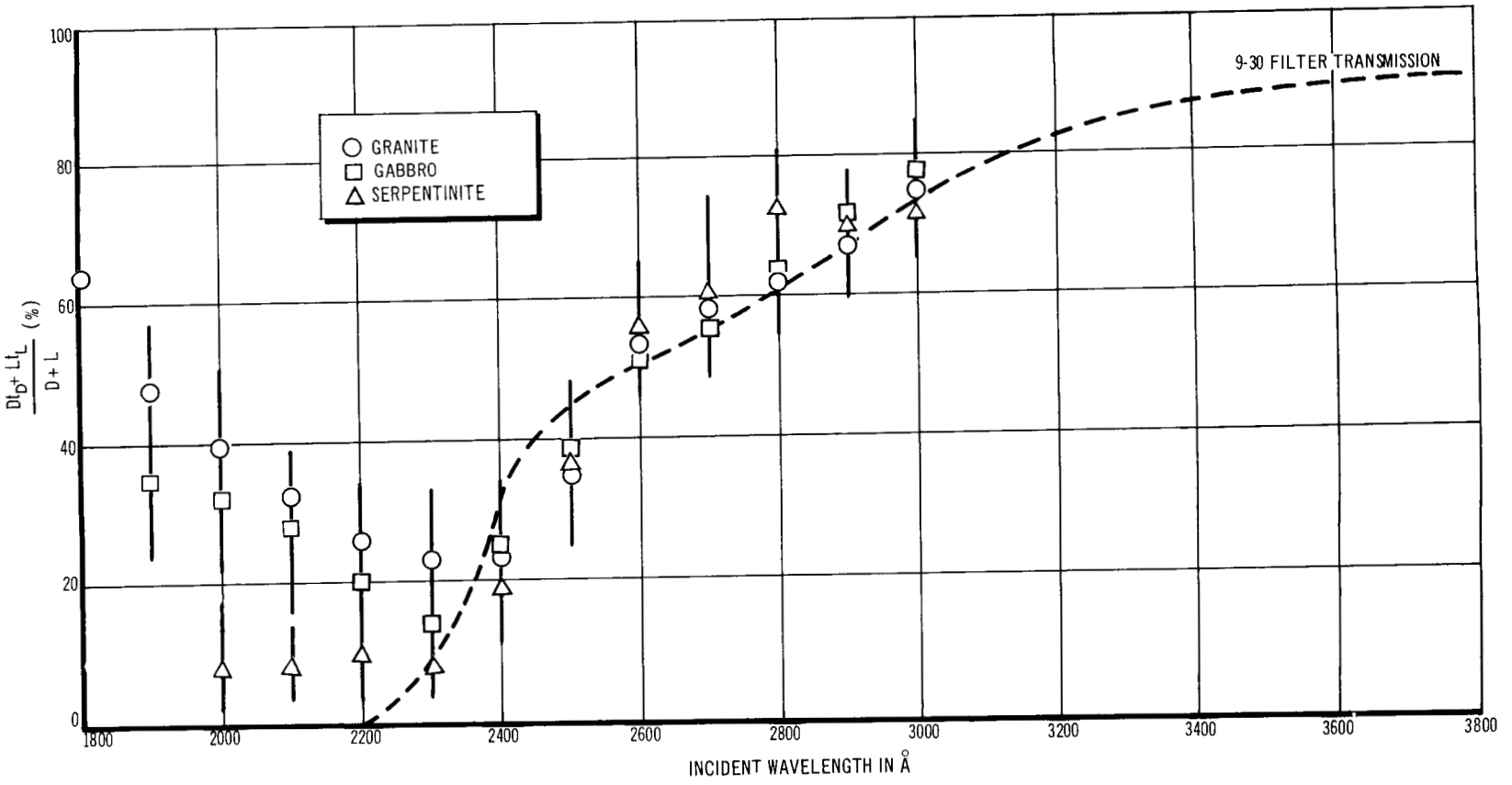

Figure 8 Transmission of Diffuse Reflection Plus Luminescence Through 9-30 Filter

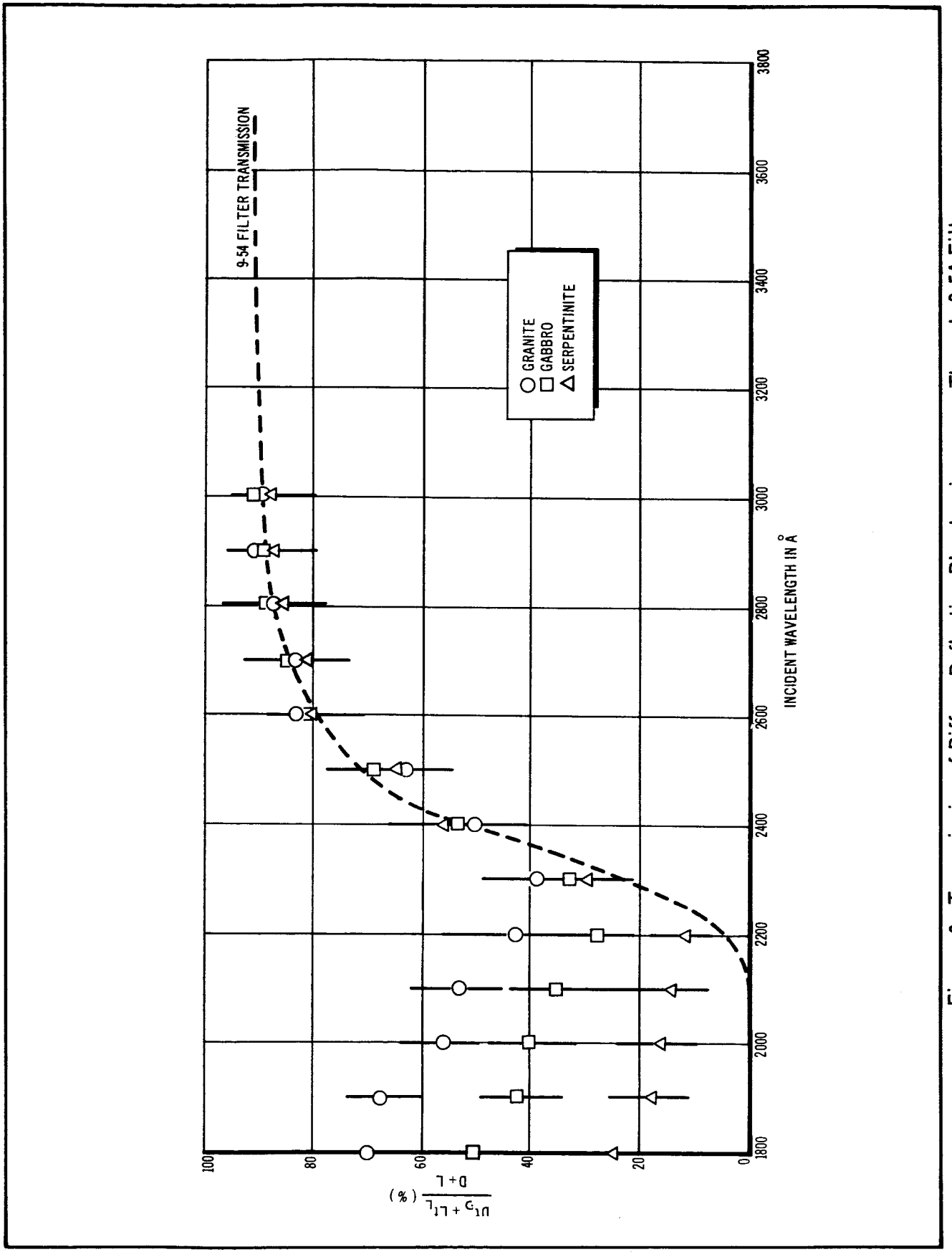

Figure 9 Transmission of Diffuse Reflection Plus Luminescence Through 9-54 Filter

where D and t_D are at the incident wavelength and L and t_L are at some longer wavelength (of course, L may cover a range of wavelengths so that t_L here can be taken as an average over this range). The results of these measurements are shown in Figures 6, 7, 8, and 9.

The results are interpreted as follows:

Serpentinite. —At incident wavelengths longer than 2300 Å the ratios for all four filters follow the transmission curves within the limits of experimental error. It is deduced that only reflection occurs for incident wavelengths 2300 Å and longer. But for incident wavelengths 1800-2200 Å, where $t_D = 0$ for all the filters, some light is detected. The ratios for pyrex and 7-54 are so small (<2%), it is concluded that there is essentially no luminescence in the wavelengths longer than 2500 Å. But the 16% ±6% through 9-54 and the 8% ± 6% through 9-30 suggest luminescence in the 2200-2400 Å region.

For 2000 Å incident and for luminescence at about 2300 Å only, $t_D = 0$ and the filter ratio is $L\, t_L/D+L$.

Using minimum values to give conservative estimates, we have

filter	t_L	$\frac{L}{D+L}\, t_L$	$\frac{L}{D+L}$
7-54	0.02	0	-
9-30	0.10	0.02	0.20
9-54	0.25	0.10	0.40
pyrex	0.00	0	-

This gives an average value of about 30% for L/D+L calculated from the 9-30 and 9-54 values. Therefore, if all the luminescence from incident 2000 Å occurs at 2300 Å, this comprises about 30% of the apparent reflectance. Since the apparent reflectance is about 4% of the incident light for serpentinite at 2000 Å, the luminescence is about 1% of the incident light.

Several measurements were made with the polished sample, with and without vacuum. With the instrument evacuated it was possible to extend the measurements down to 1800 Å incident wavelength. When measured, the 8μ powder gave results similar to the polished sample.

Granite.— The total amount of luminescence appears to be larger for granite than that arising from serpentinite. Again, for incident wavelengths longer than 2300 Å, the filter ratios follow the four filter transmission curves, showing that only wavelengths shorter than 2300 Å produce luminescence.

From the fact that a pyrex ratio of about 30% occurs with 2000 Å incident, it is concluded that some of the luminescence is at wavelengths longer than 3000 Å. The ratio of only 2% with the 7-54, which cuts off at about 4000 Å, indicates that these wavelengths are also longer than 4000 A. In addition, a second luminescent peak in the 2200-2400 A region is indicated by the 10% difference in ratio with 2000 Å incident between the 9-30 and the 9-54 because for wavelengths longer than about 3500 Å the transmissions of the two are the same.

For the case of two luminescent peaks, the filter ratio is

$$\frac{Dt_D + L_1 t_{L_1} + L_2 t_{L_2}}{D + L_1 + L_2}$$

Assume L_1 at 2300 Å:	pyrex $t_L = 0$	L_2 at 4000 Å:	pyrex $t_L = .9$
	7-54 $t_L = .02$		7-54 $t_L = 0$
	9-30 $t_L = .10$		9-30 $t_L = .9$
	9-54 $t_L = .25$		9-54 $t_L = .9$

Also, for 2000 Å incident, $t_D = 0$ for all filters.

Using conservative values, we have

pyrex

$$\frac{L_2 t_{L_2}}{D + L_1 + L_2} = 0.30 \quad \therefore \quad \frac{L_2}{D + L_1 + L_2} = 0.33, \text{ or } 33\% \text{ at } 4000 \text{ Å}$$

9-54

$$\frac{L_1 t_{L_1} + L_2 t_{L_2}}{D + L_1 + L_2} = 0.40; \quad \therefore \frac{L_1 t_{L_1}}{D + L_1 + L_2} = 0.10, \text{ and } \frac{L_1}{D + L_1 + L_2} = 0.40$$

9-30

$$\frac{L_1 t_{L_1} + L_2 t_{L_2}}{D + L_1 + L_2} = 0.32; \quad \therefore \frac{L_1 t_{L_1}}{D + L_1 + L_2} = 0.02, \text{ and } \frac{L_1}{D + L_1 + L_2} = 0.20$$

or, averaging the 9-54 and 9-30 results, about 30% of the apparent reflection is luminescence at 2300 Å.

With 30% luminescence at 2300 Å and 33% at 4000 Å, only approximately 40% of the apparent reflection is actual reflection. Since the apparent reflection is about 5% of the incident light, the luminescence is about 3% of the incident light. (It may be that the difference between the 9-30 and 9-54 filter ratios is experimental rather than real. In this event, all the induced luminescence is in the visible where the transmission of 9-54, 9-30 and pyrex is 0.9. The average of the measured ratios for these three filters with 2000 Å incident is about 0.30, indicating about 33% luminescence or approximately 1-1/2% of the incident light.)

There could, of course, be more than two peaks, but, with these four filters and the uncertainties in the values due to very low light signals, no further information can be determined.

Gabbro.— The results are similar to those of granite although the total luminescence is slightly less. Again, the pyrex and 7-54 results indicate some luminescence at wavelengths longer than 4000 Å, and the difference between the 9-54 and 9-30 results indicates luminescence also in the 2200-2400 Å region. The uncertainty in the results is sufficiently large so that no quantitative conclusions can be drawn. Calculations similar to those for granite (2000 Å incident, L_1 at 2300 Å, L_2 at 4000 Å) are as follows:

pyrex

$$\frac{L_1 t_{L_1} + L_2 t_{L_2}}{D + L_1 + L_2} = 0.23; \quad \frac{L_2}{D + L_1 + L_2} = 0.25$$

9-54

$$\frac{L_1 t_{L_1} + L_2 t_{L_2}}{D + L_1 + L_2} = 0.32; \quad \frac{L_1 t_{L_1}}{D + L_1 + L_2} = 0.09; \quad \frac{L_1}{D + L_1 + L_2} = 0.36$$

9-30

$$\frac{L_1 t_{L_1} + L_2 t_{L_2}}{D + L_1 + L_2} = 0.25; \quad \frac{L_1 t_{L_1}}{D + L_1 + L_2} = 0.02; \quad \frac{L_1}{D + L_1 + L_2} = 0.20$$

The average of the 9-54 and 9-30 results gives 30% at 2300 Å, and pyrex gives 25% at 4000 Å. The apparent reflection of gabbro at 2000 Å is about 5% of the incident light. The luminescence is, therefore, about 2% of the incident light.

For both granite and gabbro, the 8 μ powder gave slightly lower luminescence than the polished samples but with overlapping error bars. Since there was no clear distinction between the solid and the finest powder, the other powders were not run.

As far as distinction among the rock types is concerned, the luminescence detected by this technique appears to be at approximately the same wavelengths for all three rocks. Granite and gabbro both appear to have a luminescent peak of wavelength longer than 4000 Å and all three rocks have a peak near 2300 Å. They differ, however, in intensity. The intensity of granite seems to be the greatest, closely followed by gabbro, with serpentinite the least in intensity of the three.

Interestingly, the above calculations show the luminescence at 2000 Å incident to be of intensity comparable to the diffuse reflection. Attempts to detect luminescence when the sample was rotated so that the specular peak fell on the detector, however, were unsuccessful because of the greatly increased background of reflected light.

The luminescence induced by incident wavelengths shorter than 2200 Å may be responsible for the leveling off in reflectance at these wavelengths detected in the Cary measurements. As in the Tropel, the Cary will record not only the reflected light but also any induced luminescence. The actual reflectance at these shorter wavelengths may drop more rapidly than has been assumed but the addition of luminescence may cause the curve to flatten or even rise at the short wavelength end.

Summary of Ultraviolet-Excited Luminescence. —On the basis of the data described in the text, these tentative conclusions are drawn: (1) only incident wavelengths below 2200 Å produce luminescence, (2) granite shows the highest total luminescence with one peak near 2300 Å and another in the visible, (3) gabbro, with slightly less luminescence also has a visible and a 2300 Å peak, (4) serpentinite has the least total luminescence, all of it at approximately 2300 Å, and (5) approximate luminescence efficiencies for excitation in the 1800-2200 Å region are:

	2300 Å Peak	Visible Peak
Granite	1-1/2%	1-1/2%
Gabbro	1%	1%
Serpentinite	1%	

X-Ray-Excited Luminescence

The source of x-rays for these experiments was a General Electric XRD-6 x-ray fluorescence spectrometer. The x-ray tube for this instrument is a high intensity source, with a chromium target, with up to 90 mA current and 30 kV. The use of a chromium target and the relatively low voltage reduces problems of shielding and background.

In order to check the effect of voltage and current on the excited luminescence, measurements of total luminescence were made with a 1P28 photomultiplier tube. Samples were placed in the regular sample holder of the spectrometer, and the photomultiplier tube was placed at the measuring port. The results of total luminescence measurements are shown in table 4.

The order of intensity for the three rocks is the same as for the electron and proton luminescence. The decrease in intensity with decreasing particle size appears to be a function of total luminescence intensity; granite shows the greatest decrease and serpentinite shows none at all. Even at the smallest size, however, there is a five-fold intensity difference between granite and gabbro on the one hand and serpentinite on the other. The table also shows that an approximately linear relationship exists between total intensity and x-ray tube current.

The tube voltage was varied to ascertain its effect on the readings. The results of these measurements are shown in table 5.

TABLE 4

TOTAL LUMINESCENCE WITH 15 kV CHROMIUM X-RAYS

Tube Current, (mA)	Solid	590μ	44μ	8μ
Granite				
9.5	80	32	13	8.0
18	145	61	25	18
Gabbro				
9.5	43	28	15	8.3
18	77	53	30	14
Serpentinite				
9.5	1.5	1.3	1.8	1.6
18	2.8	2.6	3.2	3.0

TABLE 5

EFFECT OF X-RAY TUBE VOLTAGE ON LUMINESCENCE
(Solid serpentinite; tube current 9.5 mA)

Tube Voltage, (kV)	Luminescence Plus Background	Background	Luminescence
15	1.7	0.038	1.7
30	6.3	4.1	2.2
60	25.0	8.6	16.4

Background was measured by putting an opaque piece of paper in front of the photomultiplier tube.

These results indicate a much greater increase with voltage than with current. The background increases at an even greater rate. Because of this, 30 kV was selected as the optimum tube voltage. The maximum current with this voltage (90 mA) was used to obtain maximum luminescence in the spectral measurements.

The sample arrangement, modified for the spectral measurements, is shown in figure 10A. The samples were placed in the sample chamber supported by the holder used for electron-excited luminescence measurements. A Gaertner quartz-prism monochromator was placed against the chamber with the entrance slit two inches from the sample. An EMI 9502S photomultiplier tube was placed directly against the exit slit. Both the entrance and exit slits of the monochromator were set at 0.4 mm. Measurements were made from 2000 Å to 6000 Å. They were uncorrected for the bandpass of the Gaertner because in the 2000-3000 Å region the bandpass is reasonably small and the uncorrected curves are adequate for sample-to-sample comparisons. With entrance and exit slits at 0.4 mm. the bandpass, $\Delta\lambda$, is

$$\Delta\lambda\,(\text{Å}) = 4.4 \times 10^{-9}\ \lambda^3\ (\text{Å})$$

This gives values of 35 Å, 120 Å, and 950 Å at wavelength settings of 2000 Å, 3000 Å, and 6000 Å, respectively.

The spectra are shown in figures 11, 12, and 13. On all of the samples, the signal at wavelengths shorter than 3000 Å was of the order of the noise in the detector so that the luminescence intensity is below the sensitivity level of this equipment. At longer wavelengths, however, it is interesting to note that all the spectra show peaks at 3400 and 3600 Å. A peak at 4300 Å seems to be particularly characteristic of serpentinite. There is no evidence for this peak in the other samples.

Because the 3400 and 3600 Å peaks in some of the spectra are so sharp, it is likely that they are due to line emission from an element common to the three samples. The fact that the relative intensity is approximately the same for all samples would also tend to indicate that a single element is causing both lines. In addition, this similarity of intensity suggests that some characteristic of the x-rays might tend to excite this element in preference to others. The Kα radiation from the chromium target is very efficient in exciting the K absorption edge of titanium. To check this, a sample of 44μ gabbro was run using x-rays from a platinum target. The results of these measurements are shown in figure 14. The curve is almost identical to that given by the chromium target, which indicates that no spectral differences exist due to varying x-ray energies. The fact that the lines do not seem to be a function of the absorption edge casts some doubt on the possibility that these are due to titanium. It should be noted that the major elements present in all three rocks are magnesium, iron, silicon, and oxygen, but the identification of these apparent lines will require further investigation.

Differences are evident in the curves both with respect to rocks and to grain size. The intensity relationships that appeared in the total luminescence measurements also appear in the spectra, although the grain size effect is less marked in the spectra than in the total. Except for a shifting of one of the broad granite peaks with grain size, the shape of the curve for all four samples of each rock type is essentially the same. The chief difference is that the broad "continuum" appears to decrease more sharply than the element peaks. This is shown by sharper contrast of these peaks on the less intense spectra of the finer grain sizes of granite and gabbro and by the additional

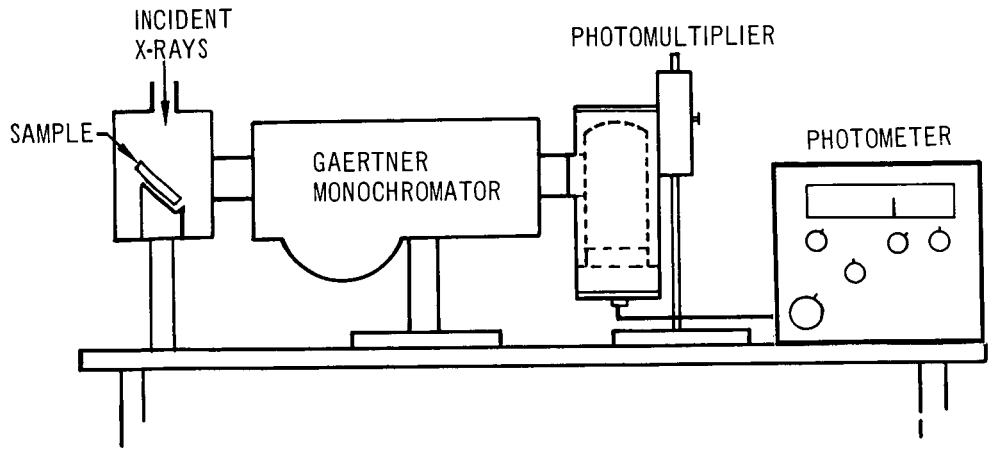

(A)

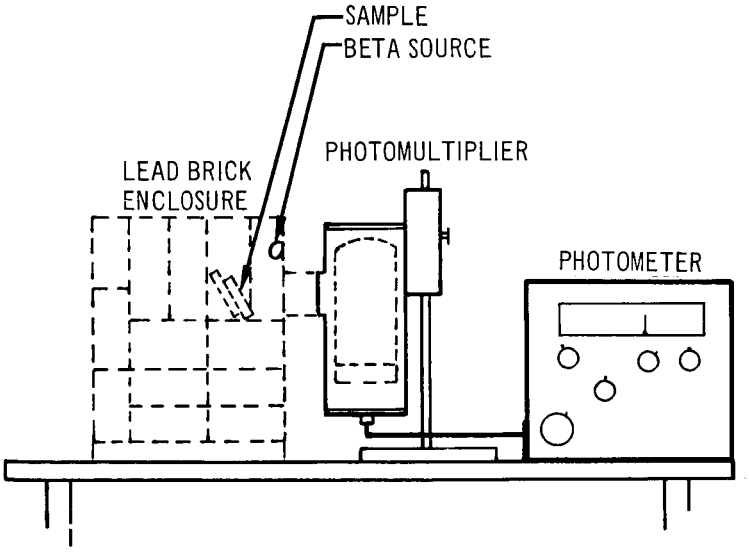

(B)

Figure 10 Instrument Arrangement for Measuring Luminescence; (A) X-Ray Excitation, (B) Electron Excitation

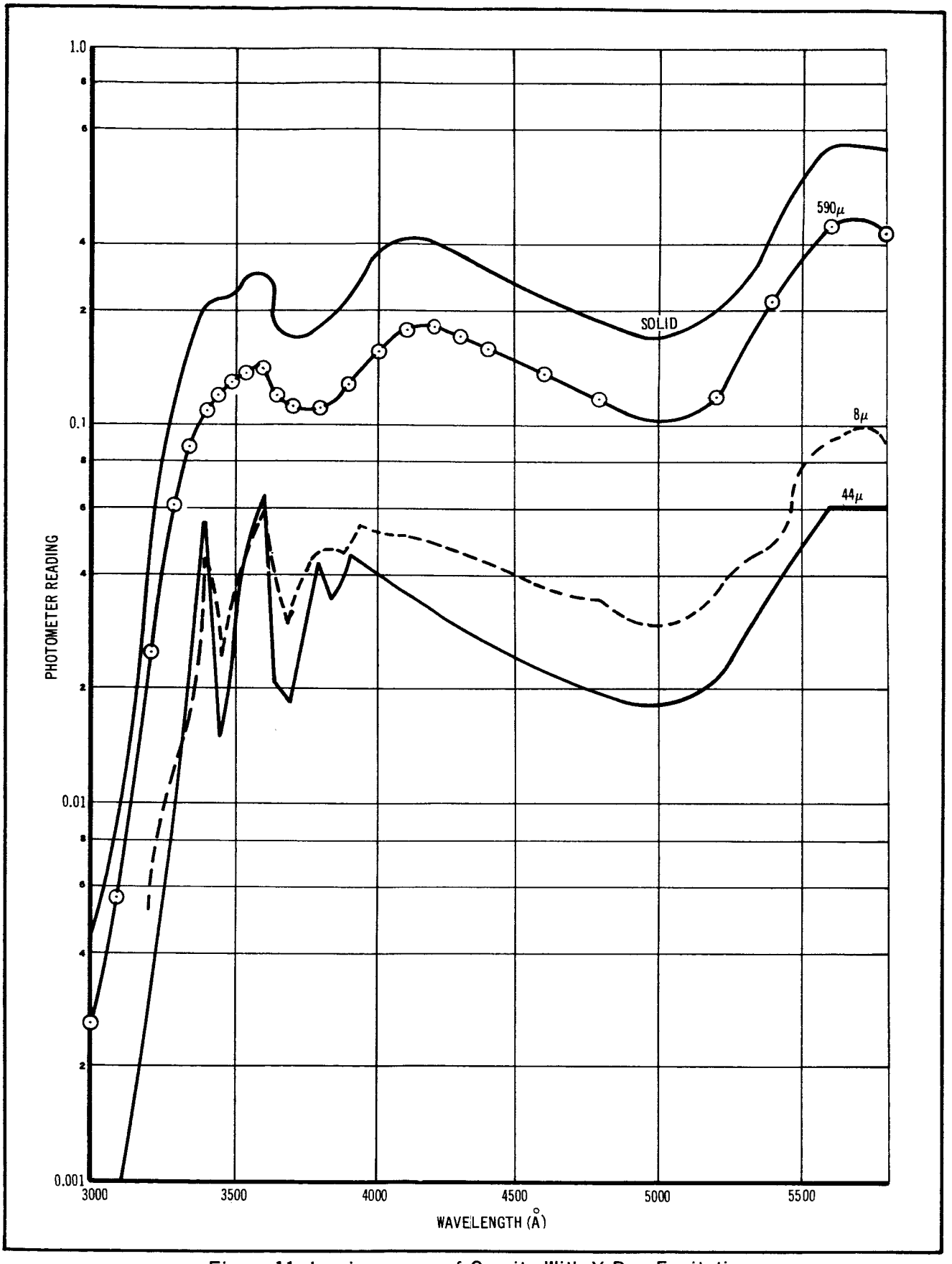

Figure 11 Luminescence of Granite With X-Ray Excitation

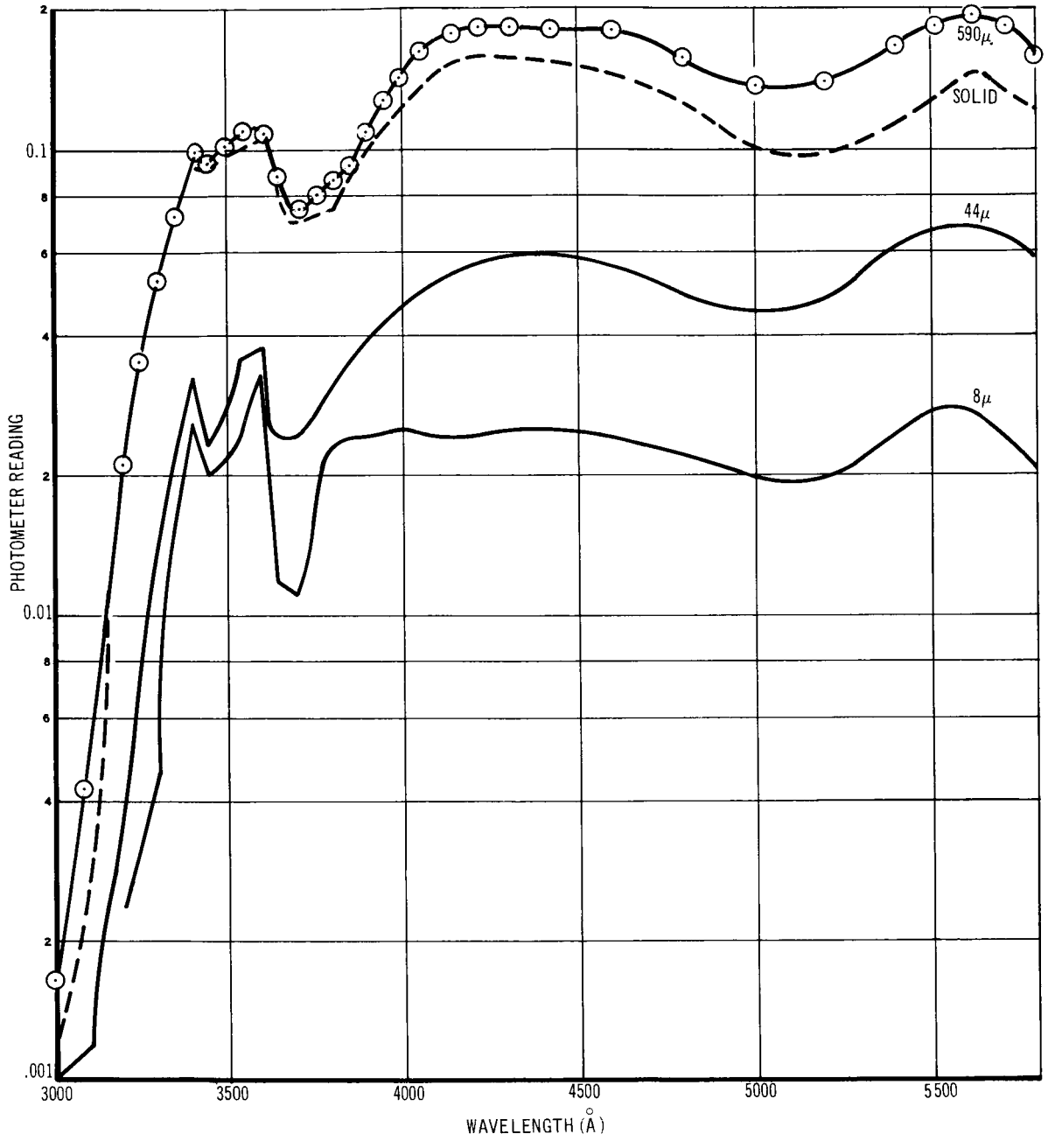

Figure 12 Luminescence of Gabbro With X-Ray Excitation

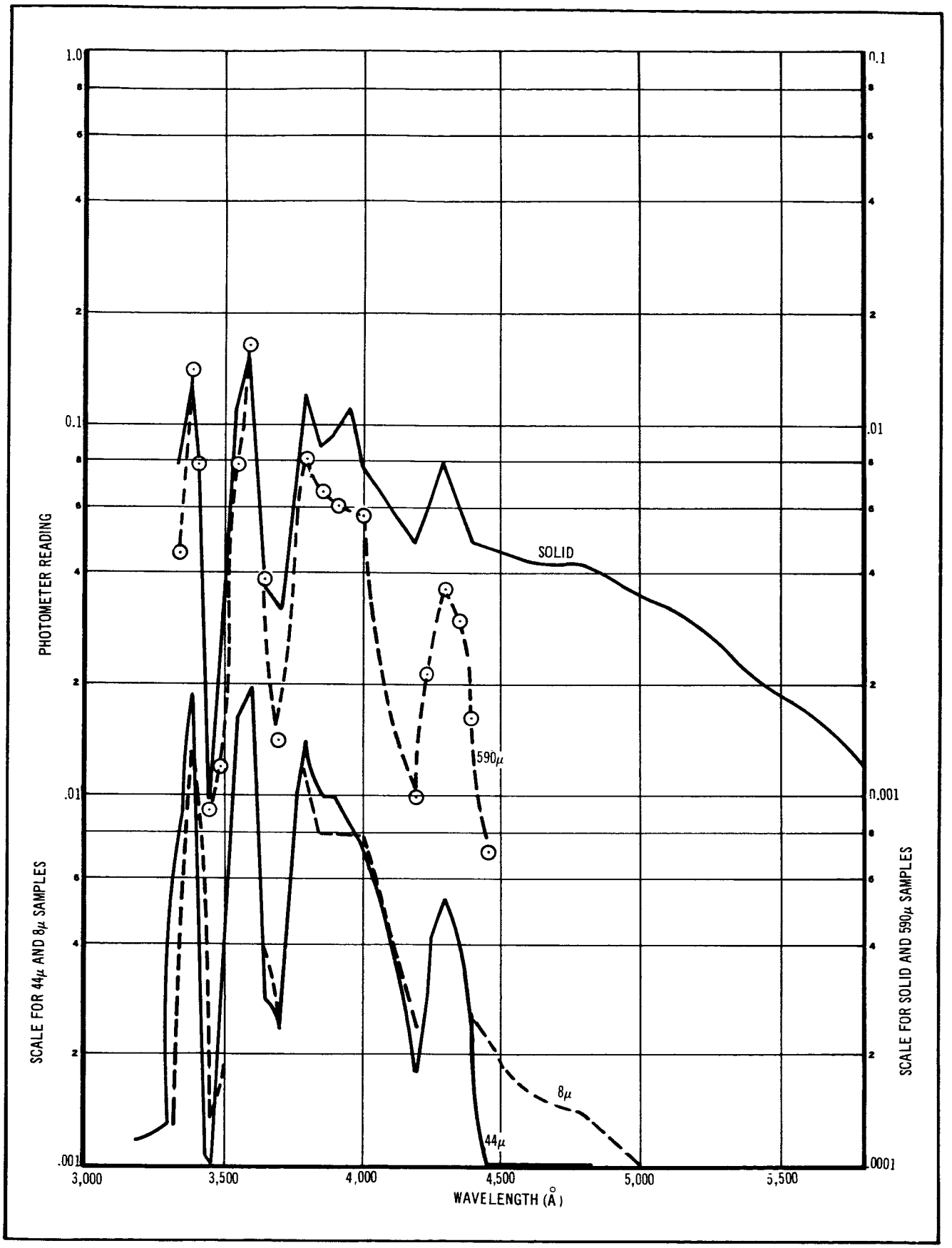

Figure 13 Luminescence of Serpentinite With X-Ray Excitation

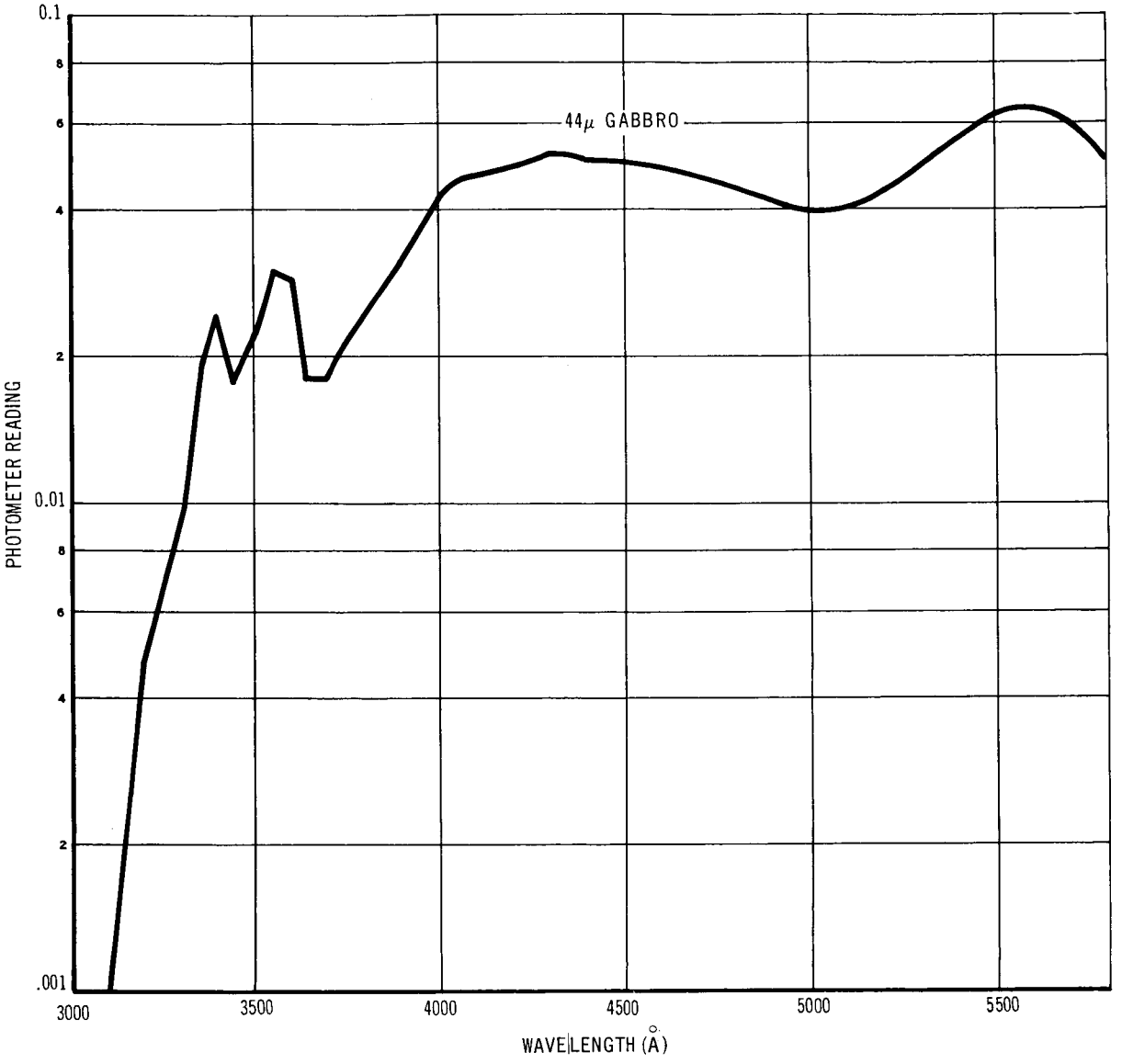

Figure 14 Luminescence of 44μ Gabbro With X-Ray Excitation From Platinum Target

peaks of this type shown in the serpentinite curves, all of which are of low intensity relative to granite and gabbro.

Calibration.—The equation given by Compton and Allison (1964) is used to estimate the output of the x-ray tube as follows:

$$\begin{aligned}\text{Efficiency} &= (\text{Atomic Number})(\text{Voltage})(1.1 \times 10^{-9}) \\ &= (24)(3 \times 10^{4})(1.1 \times 10^{-9}) \\ &= 7.9 \times 10^{-4}\end{aligned}$$

This value of efficiency gives an x-ray flux of 2.3×10^{7} ergs/sec. The sample is 5 cm from the target, so that the flux at the sample is 1.4×10^{5} ergs/cm^2 sec.

The calibrated tungsten lamp was used to obtain absolute values of intensity by the spectrometer. To minimize the scattered light problem, the lamp was operated at its maximum temperature (2500°K), and a filter which cut out light longer than 4000 Å in wavelength was put in front of the monochromator.

The light flux at this temperature is 71.6 ergs/cm^2 sec Å. When corrections were made for geometry and for the filter, it was calculated that 0.7 ergs/cm^2 sec Å was falling on the slit. The signal recorded on the EMI photomultiplier was 60.5 μA, so that the sensitivity was 0.012 ergs/cm^2 sec Å μA. The maximum signal recorded in the x-ray luminescence measurements at 3000 Å was approximately 0.008 μA, indicating a luminescence intensity of about 10^{-4} ergs/cm^2 sec Å. Thus, for the 2000-3000 Å region, the upper limit for the luminescent energy is 1000×10^{-4}, or 0.1 erg/cm^2 sec. The efficiency of these rocks for x-rays, at least those used in these experiments, is, therefore,

$$\text{Luminescence efficiency (2000-3000 A)} < 0.1/1.4 \times 10^{5} = 7 \times 10^{-7}.$$

Summary of x-ray-excited luminescence.—The results of the x-ray excitation experiments can be summarized as follows: (1) essentially all the luminescence is in wavelengths longer than 3000 Å so far as the sensitivity of the equipment used in the experiments is concerned, (2) sharp peaks, probably due to elements, are observed in all samples at 3400 Å and 3600 Å, and additional peaks at 3800 Å and 4300 Å are observed in serpentinite, (3) the rocks differ in intensity, granite having the greatest intensity, gabbro next, and serpentinite the least, (4) decreasing intensity accompanies decreasing grain size with the amount of intensity decline being greatest for the most intensely luminescing rocks; however, even at the finest grain sizes, the intensity differences of the three rock types persist, (5) the "element" peaks appear to decline less with decreasing grain size than do the broad band "continua" of the spectral curves, (6) these peaks appear to grow

sharper with decreasing grain size, and (7) the luminescence efficiency of the three rocks in the 2000-3000 Å region, with x-ray excitation of the type used, is estimated to have an upper limit of 7×10^{-7} and is almost certainly much less.

Proton-Excited Luminescence

Experimental technique.— A Texas Nuclear Co. neutron generator was used as a source of protons. This instrument provides protons with a beam diameter of 1 inch, an energy range of 20-150 keV, and a current of up to 100 μA. A sample chamber was mounted at the end of the drift tube of the proton source. It incorporated a sample holder which oriented the sample at a 45° angle to the beam. The proton-excited luminescence was viewed through a quartz window directly above the sample at 90° to the proton beam and at 45° to the sample surface. The entrance slit of the Gaertner monochromator was placed against the quartz window of the sample chamber. An RCA 1P28 photomultiplier, with an S5 photocathode surface, was used as the light sensor at the exit slit of the Gaertner. The S5 photocathode response characteristics are summarized in table 6.

TABLE 6

SUMMARY OF S5 PHOTOCATHODE RESPONSE CHARACTERISTICS

Wavelength (Å)	Quantum Efficiency (%)	Sensitivity (A/W)
2000	0.4	0.0006
2300 - 3400	11.0	0.035 - 0.052
3400 - 5000	11.0 - 7.0	0.052 - 0.03
5000 - 6000	7.0 - 1.0	0.03 - 0.005
6000 - 6300	1.0 - 0.4	0.005 - 0.0006
6300 - 7000	0.4 - 0.04	0.0006 - 0.0002

The photomultiplier was powered with batteries, with the recommended 100 volts between dynode stages and 90 volts between dynode 9 and anode. The output signal was read out by a Keithley picoammeter, which has provision for bucking out the photomultiplier dark current. The experimental arrangement is shown in figure 15.

To provide a control for each run, an Isolite light source, consisting of a sealed phosphor excited by radioactive tritium, was used to provide a secondary light reference. This source has a brightness of about 150 microlamberts, according to the manufacturer. Its spectrum is shown in figure 16. The peak at 5200 Å was used to calibrate each rock sample run by substituting the Isolite light source for the rock sample and checking the current measurement each time at 5200 Å.

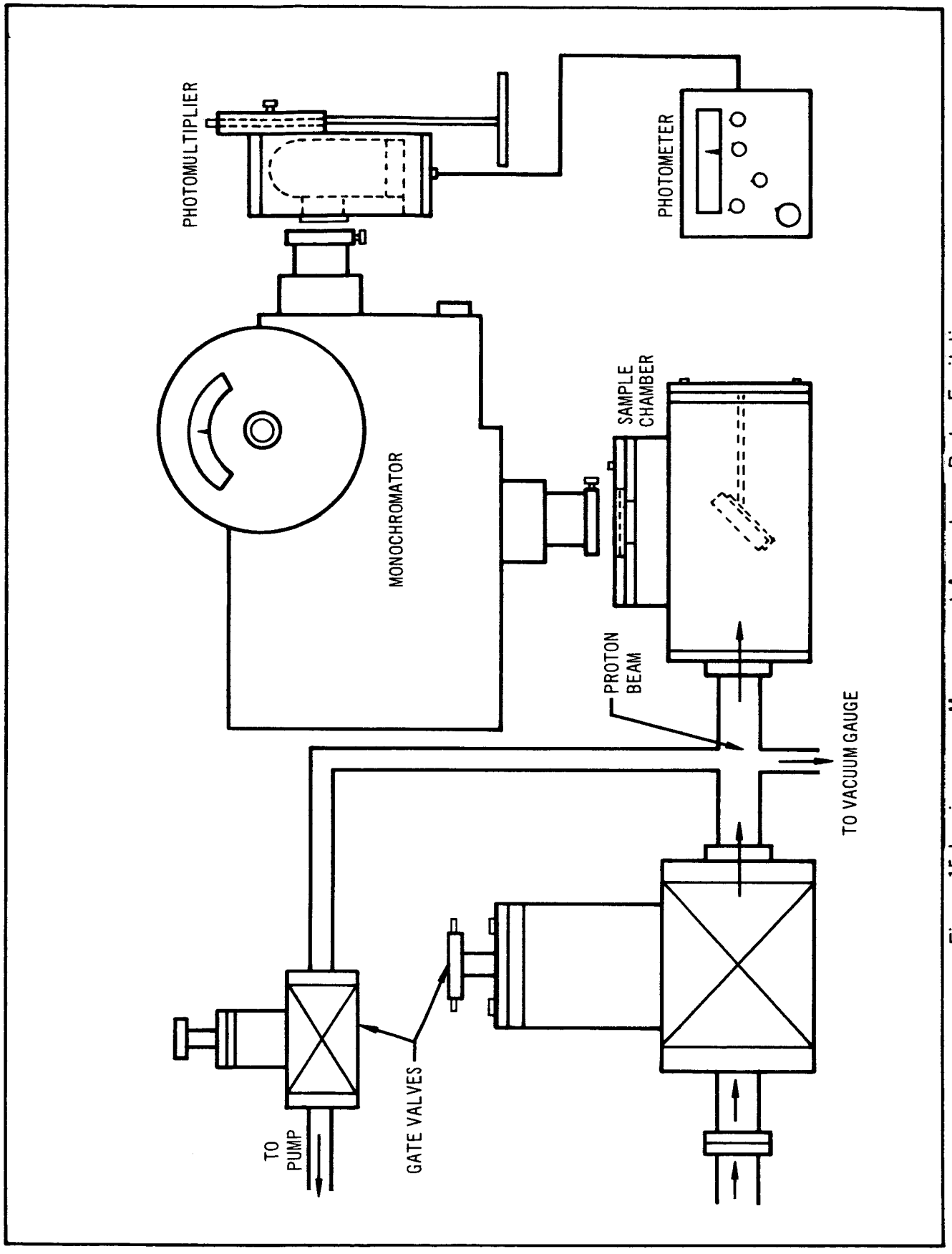

Figure 15 Luminescence Measurement Apparatus – Proton Excitation

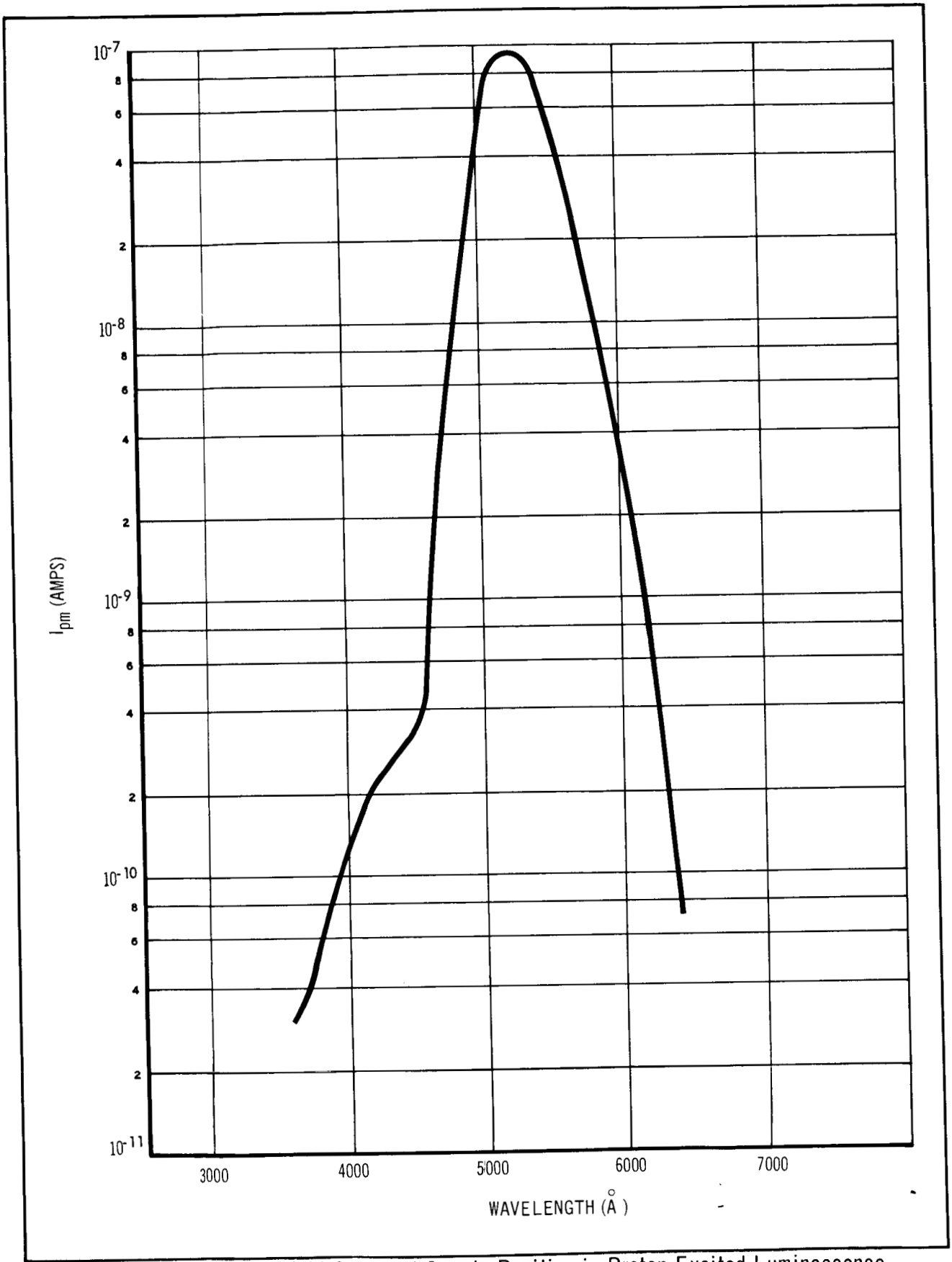

Figure 16 Isolite Light Source at Sample Position in Proton-Excited Luminescence Measuring System

Description of results.— In general, the intensity of the total luminescence from the three rock types is greatest for granite, less for gabbro, and least for serpentinite. This is shown in figures 17, 18, and 19, in which the area under the curves is representative of the total luminescence from a rock sample.

In the spectral study, the luminescence produced by the proton beam was investigated for variation with (1) rock type, (2) grain size, and (3) excitation intensity. With the absolute calibration of the measuring technique established, it was then possible to establish the efficiency of proton-to-luminescence conversion of each rock type and each grain size. The curves, as in the case of the x-ray curves, are uncorrected for bandpass and for the same reasons.

Variation with rock type.— In figures 17, 18, and 19, the spectra for granite, gabbro, and serpentinite are compared for the solid and the three powder forms of each. For each curve the proton beam consisted of 100 keV protons with a beam current of 8 μA. Differences between the three rock types can be summarized as follows:

(1) Wavelength of maximum peak:

Granite: 5400 Å (all forms)
Gabbro: 4600-4800 Å (all forms)
Serpentinite: 4600-4800 Å (all forms)

(2) Peaks between 2000-3000 Å:

Granite: 2800 Å
Gabbro: shoulder around 2800 Å
Serpentinite: 2800 Å

(3) Peaks between 3000-4000 Å:

Granite: 3400 Å
Gabbro: shoulder around 3400 Å
Serpentinite: shoulder around 3400 Å

(4) Relative amplitudes of luminescence:

Granite: highest
Gabbro: next highest
Serpentinite: lowest

(5) Plateau regions:

Serpentinite: 2500-2700 Å

As is evident, the nature of the spectra show characteristics which permit discrimination of the rock types. Relative amplitude, wavelength of maximum peak, secondary peaks in either the 2000-3000 Å or 3000-4000 Å bands, or a plateau at 2500-2700 Å provide the basis for distinction.

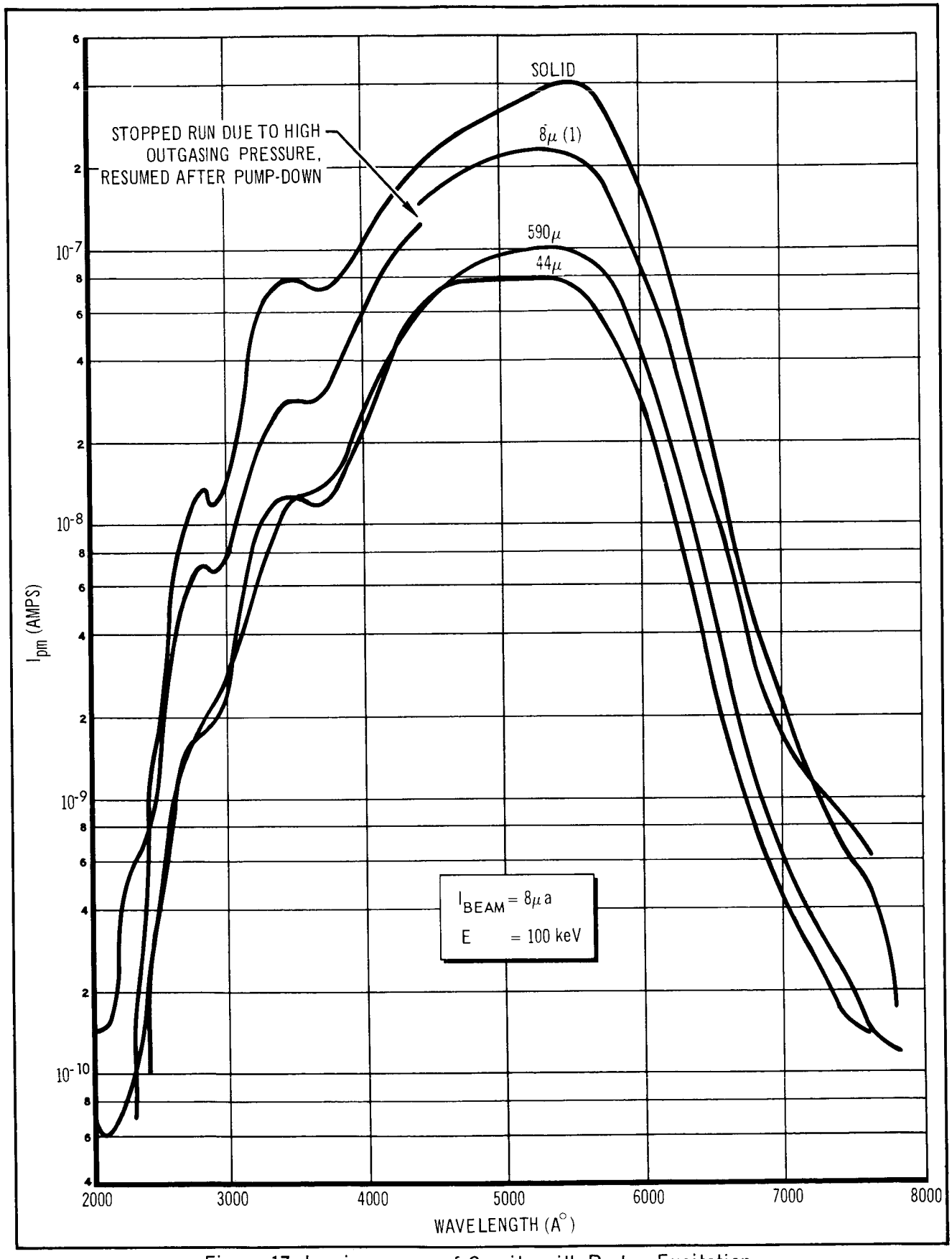

Figure 17 Luminescence of Granite with Proton Excitation

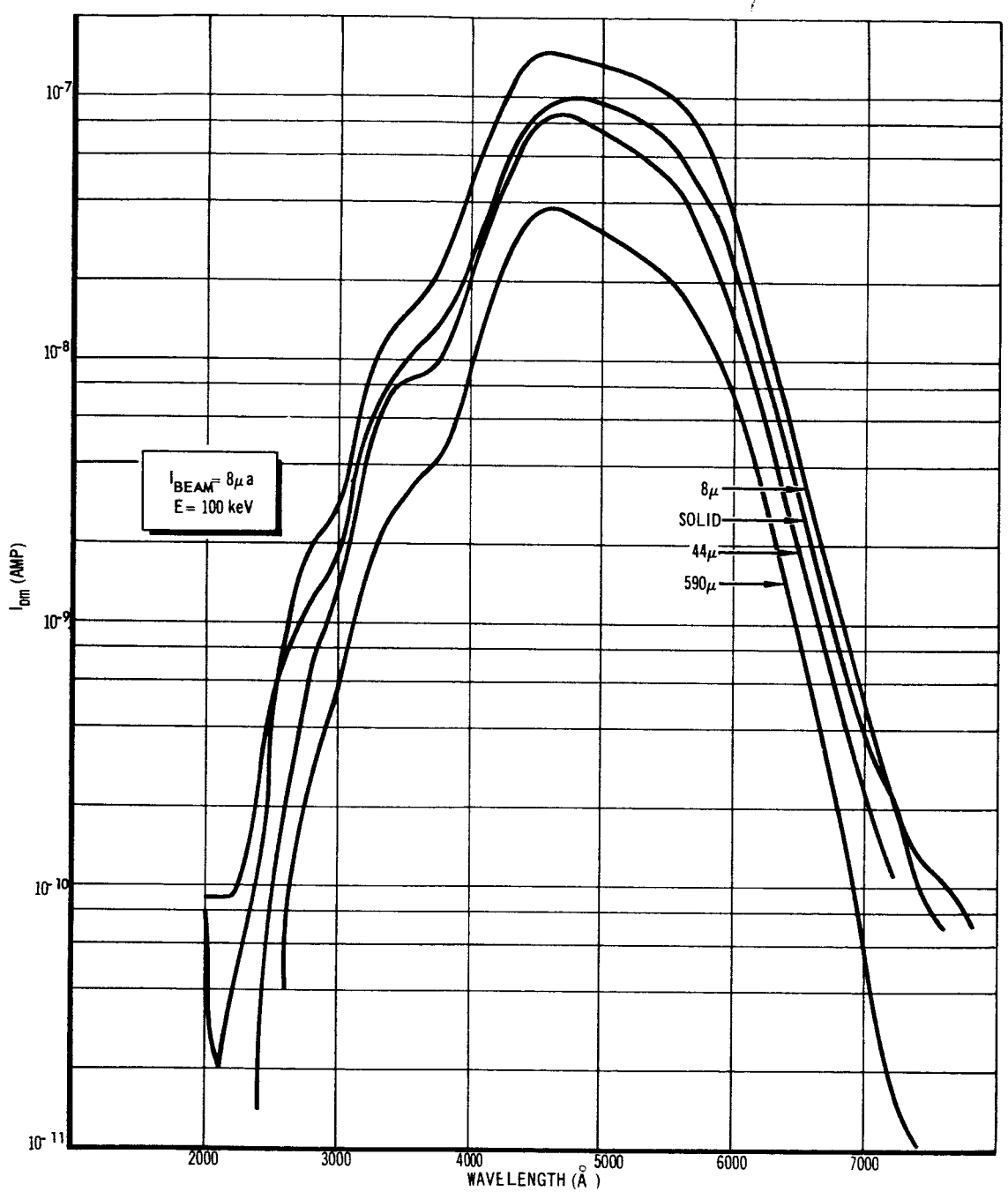

Figure 18 Luminescence of Gabbro with Proton Excitation

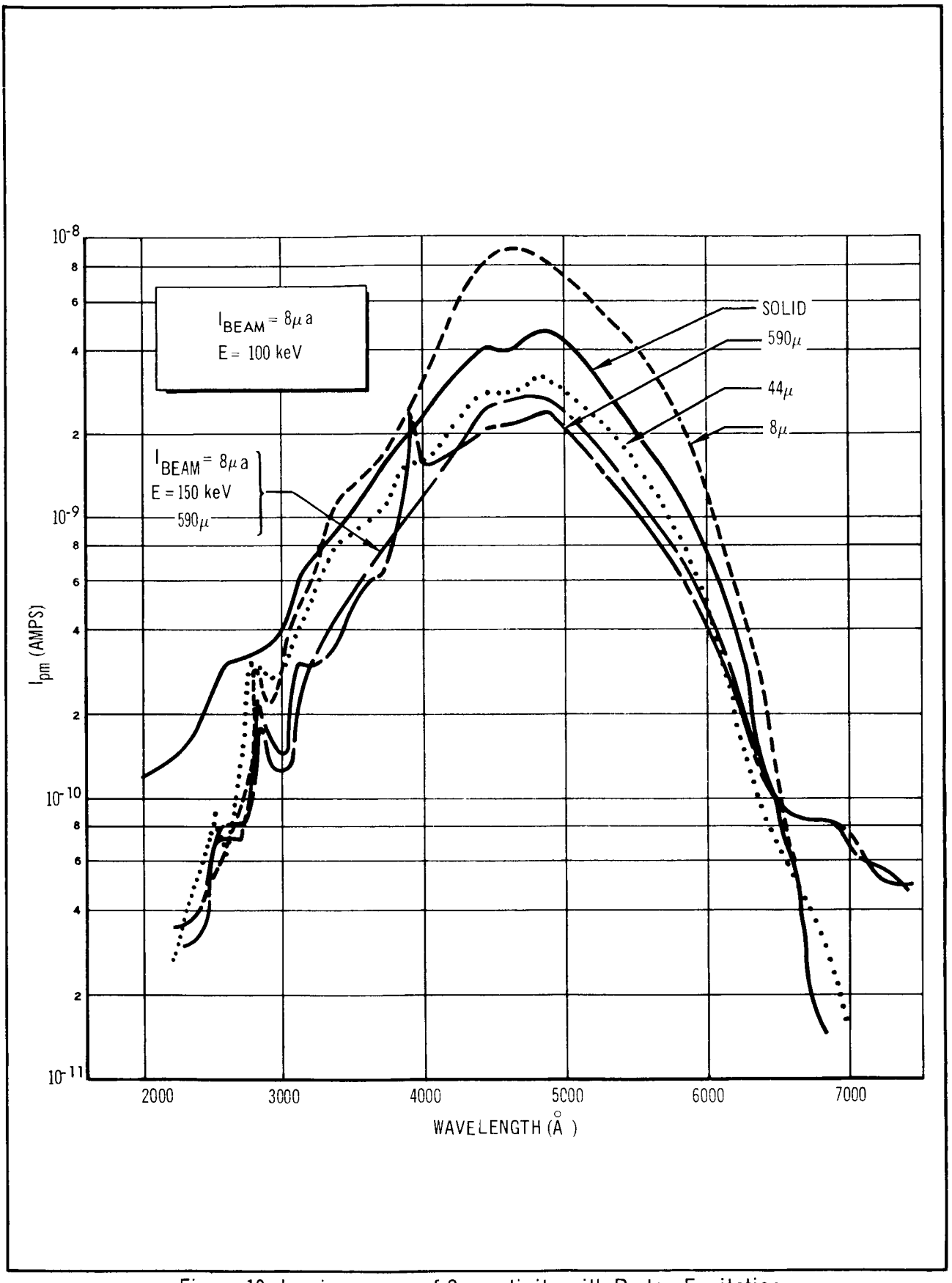

Figure 19 Luminescence of Serpentinite with Proton Excitation

Variation with grain size.— Figures 17, 18, and 19 show the variation of the spectra with grain size. For all rock types, the solid and the finest powder (8μ) are similar to each other. Also, the 590μ and 44μ powders are close to each other in characteristics. This may indicate that surface conditions of the solid and 8μ powder closely resemble each other, which would imply the same is true of the 590μ and 44μ powders as a pair. However, because the 44μ powder is more similar in grain size to the 8μ than to the 590μ powder this explanation may not hold. It is also possible that the differences are due to experimental variation — the four curves of each rock type have only a five-fold total spread in intensity. As the 8μ sample was the only one ground in a tungsten carbide ball mill, tungsten carbide contamination may account for the high intensity of that sample with respect to the others. It is not known, however, whether tungsten carbide luminesces significantly. Moreover, the 8μ sample does not show this intensity relationship with x-ray and electron excitation, although with ultraviolet excitation the solid and 8μ samples showed comparable intensities. The question should be investigated further.

Variation with excitation intensity.— The effects of proton flux density and proton energy are shown in figures 20, 21, and 22. Proton flux density was varied by using proton beam currents of 4, 8, and 16 μA, respectively, noting the effects on light output by doubling the beam current in each case. Since the beam cross-section is approximately 5.06 cm^2, the corresponding proton flux is as follows:

$$4\ \mu A = 5.03 \times 10^{12}\ \text{protons/cm}^2\ \text{sec}$$
$$8\ \mu A = 1.00 \times 10^{13}\ \text{protons/cm}^2\ \text{sec}$$
$$16\ \mu A = 2.00 \times 10^{13}\ \text{protons/cm}^2\ \text{sec}$$

The effect of varying proton energy from 100 keV to 150 keV is shown in figures 20 and 22 for granite and in figure 19 for serpentinite.

In general, the luminescent light output increases with proton flux density increase (figure 20). A linear relationship is not evident in these data but this may be due to progressive contamination of the surface in the course of successive runs, as mentioned below. Also, in general, the luminescent light output increases with proton energy increase (figures 19, 20, and 22).

It was observed in a series of successive runs on the same sample that the light output was progressively degraded. This is shown in figures 17 and 20 for granite and figure 21 for serpentinite. This may be due to the dark deposit that formed on each sample because of organic vapor traces in the system, to an actual change in the rock sample itself, or to some other undetermined cause.

The effect in the case of granite was different from that in the case of serpentinite. Comparison of the curves for 8μ granite subjected to a beam current of 8μA (figures 17 and 20) shows the degradation of light output throughout each successive curve. In addition, the spectral maximum peak appears to have shifted from 5400 Å to 4600 Å. The latter is the same maximum peak region for gabbro and serpentinite.

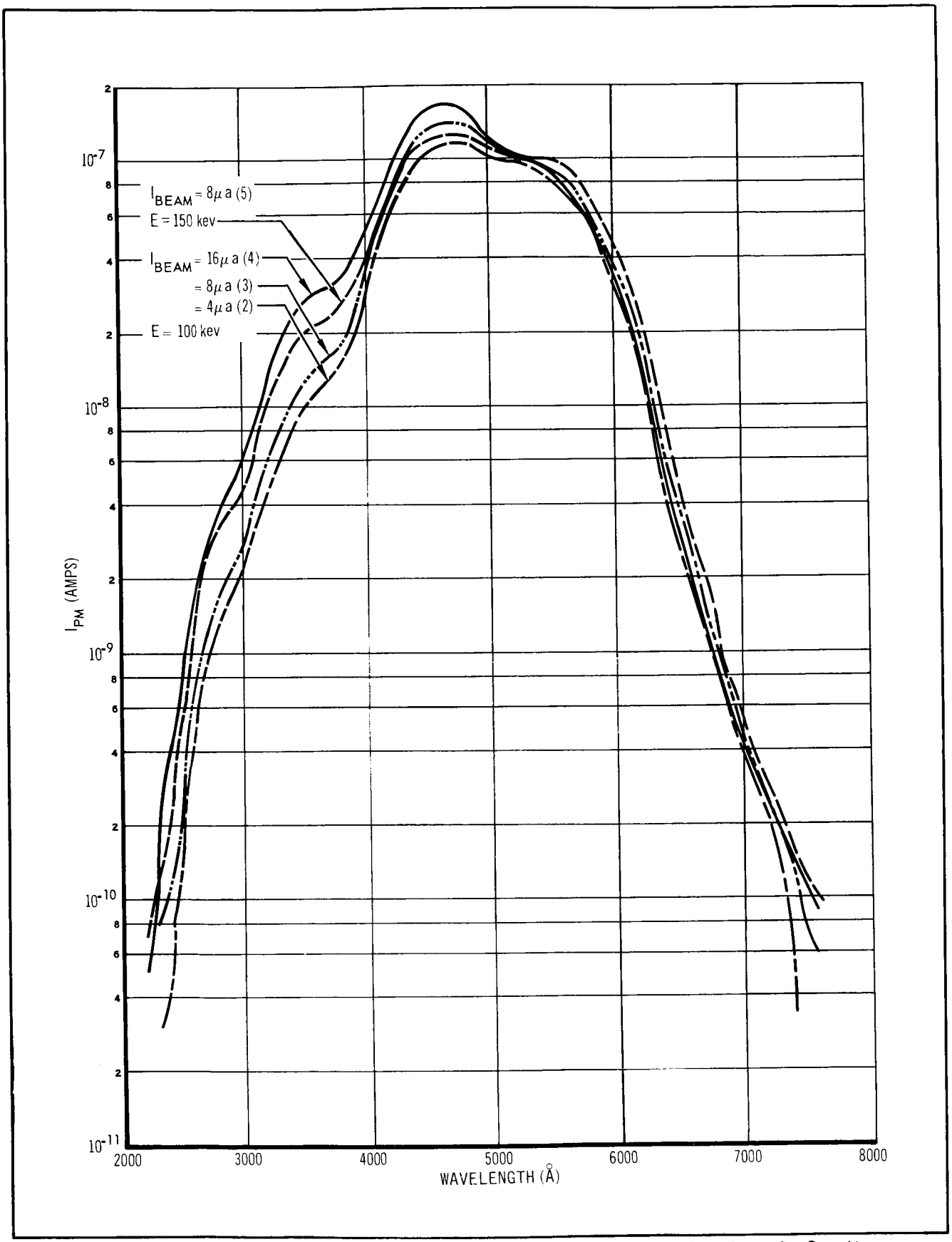

Figure 20 Variation of Proton-Excited Luminescence With Flux Density –8μ Granite

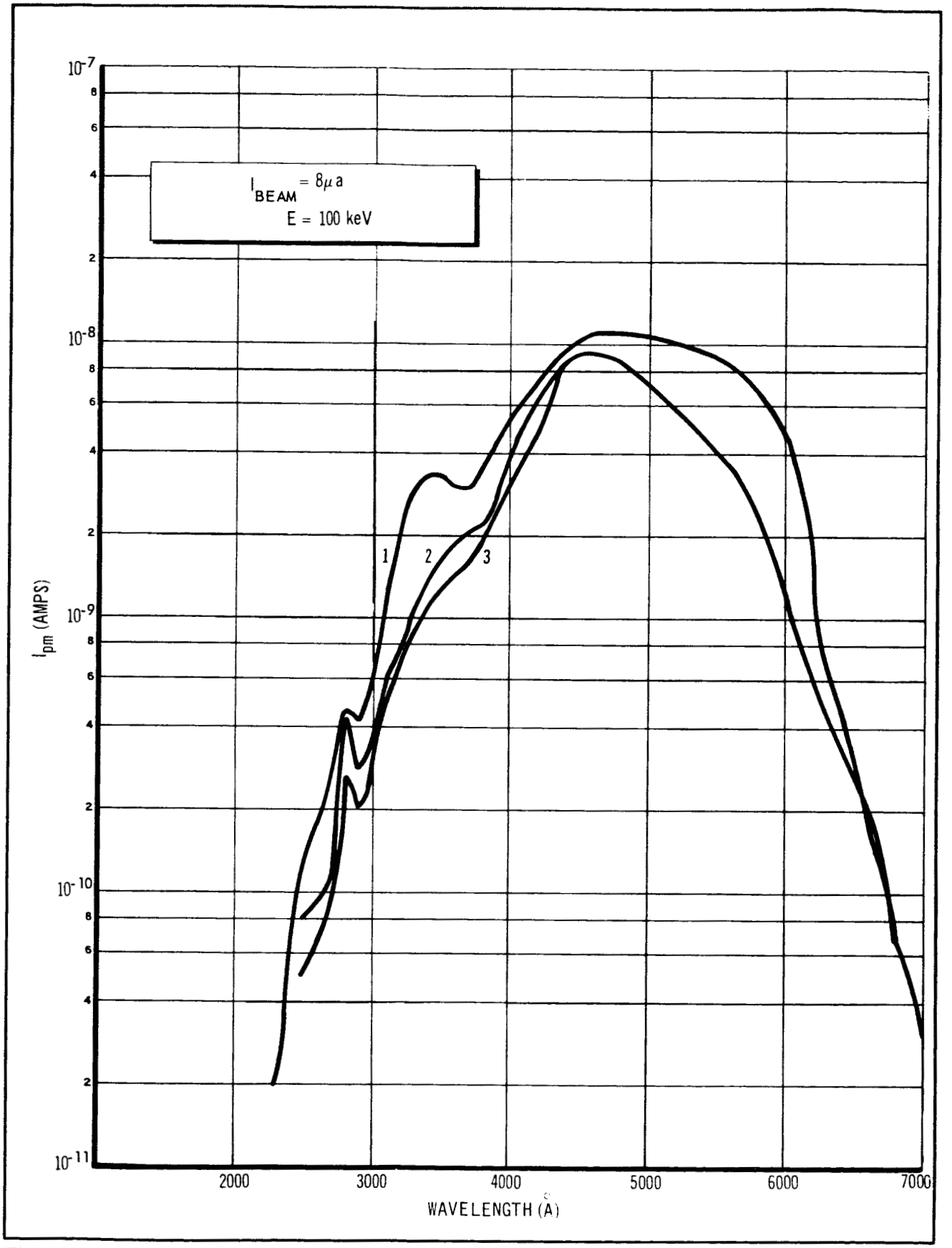

Figure 21 Variation of Proton-Excited Luminescence in Three Successive Runs with 8 μ Serpentinite

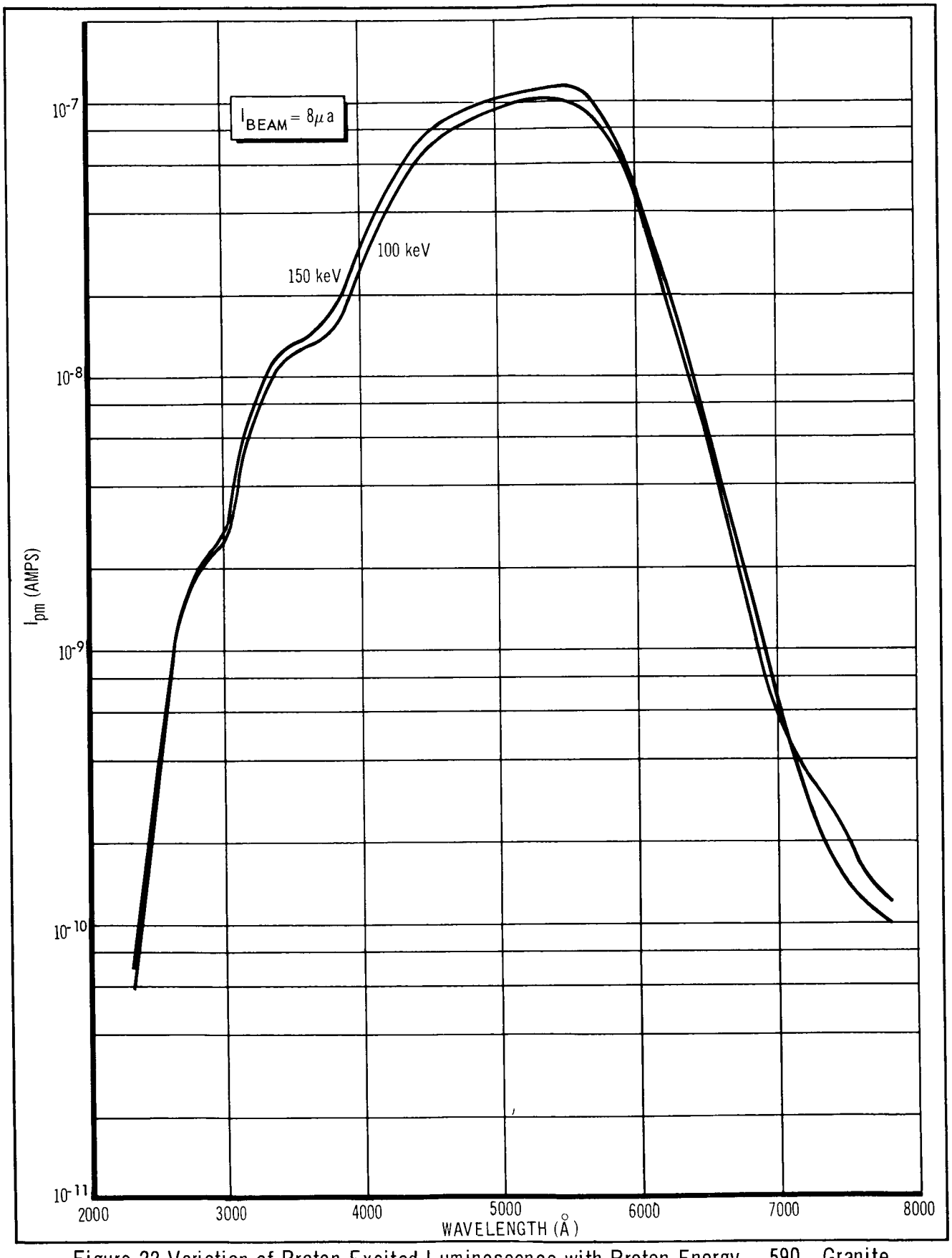

Figure 22 Variation of Proton-Excited Luminescence with Proton Energy – 590 μ Granite

It is not known, at present, whether this is a real shift or a modification of the true peak. The two curves are very similar except for a smoothing out of the characteristic granite peaks at 2800 Å and 3400 Å and an apparent "chopping off" of the maximum peak starting at 4600 Å and continuing into the longer wavelength region.

This effect appears to be a progressive one. Each curve for the 8μ granite in figures 17 and 20 is identified in the key with a number in parenthesis. This number gives the chronological order in which the measurements were made. The slope of the "chopped off" maximum peak can be observed to steepen with successive runs, but the apparent maximum peak remains at 4600 Å. The overall amplitude likewise degrades as previously described.

If the carbonaceous deposit is responsible for this change, it is producing the observed effects either by absorption or emission or both. It is interesting that fresh and clean samples of granite show the characteristic curves of figure 17. The "chopping off" seems to indicate that a process of absorption by the deposit is responsible. This would also be consistent with the overall amplitude degradation that occurs as the deposit builds up. In other words, the true properties of the granite become masked by the carbon deposit. If the carbon or organic vapor luminesces, this could override the granite emission, and the peak at 4600 Å could be that of the foreign matter rather than of the rock. Resolution of this question requires further investigation. No major pressure changes were observed to indicate significant outgasing of the granite powder. Hence, it is not likely that a change in the rock is responsible.

The case of the 8μ serpentinite powder is slightly different. Figure 21 shows the progressive degradation in overall amplitude in three successive runs. Much outgasing occurred during the first run, causing a three-fold pressure increase while succeeding runs showed no significant change in pressure. Because of exhaustion of the hydrogen gas supply to the ion source, it was necessary to stop the second run at 4400 Å and re-start with the third run.

It is evident that the peak at 2800 Å remains, the peak at 3400 Å is smoothed out, and the maximum peak at 4600 Å persists. However, the "chopping off" phenomenon occurs at wavelengths longer than 4600 Å, as in the case of the granite. The pressure changes observed indicate some change in the material; however, the effect of a deposit is also evident.

Efficiency determination.– For a beam current of 8μA, a proton energy of 100 keV, and a beam diameter of one inch,

$$\text{flux} = (10^{13}\ \text{protons/cm}^2\ \text{sec})(5.06\ \text{cm}^2)(10^5\ \text{eV})(1.6 \times 10^{-12})$$

$$= 8.1 \times 10^6\ \text{ergs/sec}$$

The calibration to determine the luminescent flux from the sample was achieved by placing the Isolite light source in place of the rock sample and calibrating the signal current accordingly.

The luminous flux of the Isolite at the maximum peak of 5200 Å and a bandpass of 620 Å is 11 ergs/sec, calculated on the basis of the brightness value of 150 microlamberts supplied by the manufacturer. With this value of the flux, it was established that, in the measuring system, a signal of 5×10^{-10} amperes (a typical value for the 2000-3000 Å band) corresponds to a luminous flux of 1.3 ergs/sec for a bandpass of 70 Å. Table 7 summarizes the efficiency measurements for the study samples.

Summary of proton-excited luminescence.—Results of the proton excitation experiments can be summarized as follows: (1) granite shows the highest luminescence intensity, gabbro the next highest, and serpentinite the least, (2) for grain size, the order of intensity, from highest to lowest, is: 8μ, solid, 44μ, 590μ, except for granite, for which the order is: solid, 8μ, 590μ, 44μ, (3) the identifying peaks of granite are: 5400 Å (maximum), 3400 Å, and 2800 Å, (4) the identifying peaks of gabbro are: 4600-4800 Å (maximum), shoulders at 3400 Å and 2800 Å, and a characteristic slope from 4600 Å to 5600 Å, (5) the identifying peaks of serpentinite are: 4600-4800 Å (maximum), 2800 Å, a shoulder at 3400 Å, a plateau at 2500 Å, and a possible double peak at the maximum, (6) an increase of 100% in proton flux results in an increase of about 20% in luminescent flux, (7) an increase of 50% in proton energy results in an increase of about 10% in luminescent flux, and (8) efficiencies are about 10^{-8} to 5×10^{-7} for the 2000-3000 Å region; about 5×10^{-7} to 10^{-4} for 5200 Å.

Electron-Excited Luminescence

For the electron-excited luminescence, a holder was fabricated which held the sample at a 45° angle to the horizontal. A 200 millicurie Sr-90 source was positioned vertical to the sample; it provided electrons of 2.3 MeV energy. The axis of the photomultiplier was horizontally positioned on the sample so that it could not see the Sr-90 source. A shutter arrangement on the photomultiplier made it possible to exclude light for background measurements, to measure all of the light, or to interpose a glass slide and measure only the visible component of the light. The experimental arrangement is shown in figure 10B.

The 1P28 phototube was found to be sensitive to the electrons scattered from the sample. To correct for this, the reading with the shutter closed was used as an indication of the back-scattered particles and x-rays from the sample and an appropriate ratio was applied to determine the correction to be subtracted from the open shutter reading. The value of this ratio was determined by removing the sample so that the photomultiplier saw only electrons and no luminescence and measuring the response with shutter open, shutter closed, and with a glass slide. It was found that the ratio for shutter open to shutter closed was 11.0 and for glass slide to shutter closed was 4.4. The transmission of the glass slide in the visible wavelengths was found to be 90%. Table 8 shows the corrected measurements for the experimental technique used.

TABLE 7

LUMINESCENCE EFFICIENCY WITH PROTON EXCITATION
(Proton Flux Density = 1.6×10^6 ergs/cm^2 sec)

Rock	Grain Size	Luminescence Signal (Amperes)		Luminescence Flux Density (ergs/cm^2 sec)		Efficiency	
		2500 Å	5200 Å	2500 Å	5200 Å	2500 Å	5200 Å
Granite	Solid	1.5×10^{-9}	3.5×10^{-7}	7.6×10^{-1}	1.8×10^{2}	4.7×10^{-7}	1.1×10^{-4}
	590μ	5.0×10^{-10}	1.0×10^{-7}	2.5×10^{-1}	5.1×10^{1}	1.6×10^{-7}	3.2×10^{-5}
	44μ	5.0×10^{-10}	7.8×10^{-8}	2.5×10^{-1}	3.9×10^{1}	1.6×10^{-7}	2.5×10^{-5}
	8μ	2.0×10^{-9}	2.3×10^{-7}	1.0×10^{0}	1.2×10^{2}	6.3×10^{-7}	7.2×10^{-5}
Gabbro	Solid	4.8×10^{-10}	8.6×10^{-8}	2.4×10^{-1}	4.4×10^{1}	1.5×10^{-7}	2.7×10^{-5}
	590μ	4.0×10^{-11}	2.6×10^{-8}	2.0×10^{-2}	1.3×10^{1}	1.3×10^{-8}	8.2×10^{-6}
	44μ	1.0×10^{-10}	6.4×10^{-8}	5.1×10^{-2}	3.2×10^{1}	3.2×10^{-8}	2.0×10^{-5}
	8μ	5.2×10^{-10}	1.2×10^{-7}	2.6×10^{-1}	6.1×10^{1}	1.6×10^{-7}	3.8×10^{-5}
Serpentinite	Solid	2.6×10^{-10}	3.2×10^{-9}	1.3×10^{-1}	1.6×10^{0}	8.2×10^{-8}	1.0×10^{-6}
	590μ	7.0×10^{-11}	1.6×10^{-9}	3.5×10^{-2}	8.1×10^{-1}	2.2×10^{-8}	5.1×10^{-7}
	44μ	9.0×10^{-11}	2.3×10^{-9}	4.6×10^{-2}	1.2×10^{0}	2.8×10^{-8}	7.3×10^{-7}
	8μ	1.3×10^{-11}	5.9×10^{-9}	6.6×10^{-2}	3.0×10^{0}	4.1×10^{-8}	1.9×10^{-6}

TABLE 8

TOTAL LUMINESCENCE INTENSITY WITH ELECTRON EXCITATION
(Relative Units)

Rock	Grain size	Without glass filter	With glass filter	Difference	Percent ultraviolet
Granite	Solid	23.5	16.2	7.3	31.0
	590μ	9.6	4.3	5.3	55.2
	44μ	4.8	1.9	2.9	60.5
	8μ	4.7	1.8	2.9	61.7
Gabbro	Solid	14.1	7.5	6.6	46.8
	590μ	9.6	4.3	5.3	55.2
	44μ	5.1	1.8	3.3	64.8
	8μ	5.4	1.8	3.6	66.7
Serpentinite	Solid	7.4	2.7	4.7	63.5
	590μ	5.0	2.0	3.0	60.0
	44μ	4.8	1.8	3.0	62.5
	8μ	5.3	1.4	3.9	73.6

Attempts to measure the spectrum with the Gaertner monochromator and the 1P28 phototube failed due to low total intensity. The more sensitive EMI tube was then tried, but it was found that the region of maximum response for the granite was barely above the background count. As in the case of the x-ray experiments, therefore, only an upper limit can be given for the efficiency.

With the experimental configuration used, the sample receives from the Sr-90 source a flux of about 10^8 electrons/cm^2 sec of 2.3 MeV energy, or about 370 ergs/cm^2 sec. From the calibration of the detector, already given, and from the background value, the maximum luminescence is 2.4×10^{-5} ergs/cm^2 sec Å at 3000 Å, or 0.024 ergs/cm^2 sec over the 2000-3000 Å range. The efficiency for electron excitation of these rocks under these experimental conditions is then: luminescence efficiency (2000-3000 Å) $< 0.024/370 = 6 \times 10^{-5}$. Note that this is merely an upper limit and does not imply a higher efficiency for electrons than for x-rays despite the fact that the number is larger. A higher energy flux of electrons, if it produced no detectable luminescence, would place a larger number in the denominator and lower this limit accordingly.

Summary of electron-excited luminescence. — The results of the electron-excitation experiments can be summarized as follows: (1) the solid samples of the three rocks show that granite has the highest luminescence intensity, gabbro the next, and serpentinite the least, (2) intensity decreases with decreasing grain size, the greatest decrease occurring in the rocks of highest intensity, such that at 590μ, granite and gabbro are of the same intensity but still distinguishable from serpentinite, whereas at 44μ and 8μ, the three rocks are indistinguishable, (3) the intensity decrease with decreasing grain size appears to be greater for the visible than for the ultraviolet wavelengths, and (4) the luminescence efficiency of the three rocks in the 2000-3000 Å region, with electron excitation of the type used, is estimated to have an upper limit of 6×10^{-5} and is almost certainly very much less.

FEASIBILITY EVALUATION

Lunar Ultraviolet Radiation

The intensity of the lunar radiation in the 2000-3000 Å region, made up of reflected and luminescence components, can be calculated from the experimental results of this study. This is shown in table 9 for the sunlit side and for the dark side. In the table, the 2000-3000 Å region is divided so as to bracket conveniently the 2200-2500 Å interval in which most of the ultraviolet-excited luminescence seems to occur and the 1800-2200 Å interval which, of the wavelengths used in the experiments, seems principally to excite this luminescence. Although the luminescence efficiency of 1% for ultraviolet excitation may be high and could possibly be revised downward by additional study, it gives a calculated 5% of the reflected background. This is the average observed by Grainger (1963) in his ground-based measurements of lunar luminescence at 3970 Å (range of 2% to 10% of six measurements for five different areas), so that the value is a reasonable one.

It is evident that for the sunlit side of the moon, the ultraviolet energy is the only significant excitation source for luminescence. In addition, the reflected ultraviolet energy in the entire range 1800-3000 Å greatly exceeds that from luminescence. The ultraviolet energy radiating from the dark side is due entirely to luminescence but it is extremely small in amount.

It must be borne in mind, however, that in the case of the x-rays and charged particles, high incident energies, especially on the dark side, may well exist due to interactions with the solar plasma, extension of the geomagnetic cavity, and other effects. These are discussed further on in this section of the report.

TABLE 9

LUNAR RADIATION, 1800-3000 Å

Incident Radiation	Incident Energy (ergs/cm^2 sec)	Reflectance Coefficient (%)	Luminescence Efficiency (%)	Reflected Energy (ergs/cm^2 sec)	Luminescence Energy (ergs/cm^2 sec)
Sunlit Side					
1800 - 2200 Å	700	6-1/2	1	45	
2200 - 2500 Å	2 000	7		140	7
2500 - 2800 Å	6 000	8		480	
2800 - 3000 Å	10 000	10		1000	
X-ray (1.5-8 Å)	10		<0.00007		$<7 \times 10^{-6}$
Proton	≤ 0.04-3		0.00005		2×10^{-8}-1.5×10^{-6}
Electron	10^{-8}-10^{-3} (10^{-2}?)		<0.006		$<\{6 \times 10^{-13}$ to $6 \times 10^{-8}\}$
Totals	18 700			1665	7
Dark Side					
X-ray (1.5-8 Å)	$\geq 7 \times 10^{-7}$		<0.00007		$<5 \times 10^{-13}$
Proton	$\sim 10^{-6}$ (0.04 - 3?)		0.00005		5×10^{-13}
Electron	$\sim 10^{-7}$		<0.006		$<6 \times 10^{-12}$
Totals	1.8×10^{-6}				5×10^{-13}

Energy Available at Lunar Orbiting Vehicle

Let E_R = energy per sec received by the detector on the orbiter

E = energy per cm^2 per sec emitted by the lunar surface, assumed to be diffuse and isotropic

D = area of detector aperture

h = altitude of detector above the lunar surface

a = acceptance angle of detector

A = area of lunar surface seen by detector.

Then

$$E_R = EA \text{ (solid angle subtended by detector}/2\pi)$$
$$= EA\,(1/2\pi)\,(D/2\pi h^2)\,2\pi = EAD/2\pi h^2$$

For an altitude of 80 miles or less and an acceptance angle of 30° or less, the error in neglecting the curvature of the lunar surface and calculating A as a plane surface is less than 3%. Therefore,

$$A = \pi h^2 \tan^2 a$$
$$\text{and } E_R = (ED \tan^2 a)/2$$

Thus, the energy available at the detector depends on the energy leaving the lunar surface, on the area of the detector aperture, and on the acceptance angle (or the f number, which is inversely proportional to tan a).

Detectability

The problem of detectability is two-fold. On the sunlit side of the moon, it is necessary to detect a measurable signal against a high background, whereas on the dark side, the background is absent but a very low signal must be detected. The reflected ultraviolet is not considered utilizable for compositional determination because of the essentially featureless reflectance curves and the lack of clear distinction among the rocks and grain sizes.

On the sunlit side, adequate energy is available in the 2200-2500 Å luminescence to be detected by the Tropel instrument. The Tropel calibration gives 3.2×10^{-3} ergs/cm^2 sec Å, and taking the minimum detectable signal as 0.01 μA,

$$E_R \text{ (minimum)} = 3.2 \times 10^{-3} \times 300 \times 0.01 = 9.6 \times 10^{-3} \text{ ergs/sec}$$

so that

$$E_R \text{ (minimum)} < EA/2\pi h^2$$

Therefore, the minimum area of the lunar surface that will give a detectable signal for the luminescence component of the radiation is as follows:

$$A\ (\text{minimum}) > 2\pi h^2 E_R/E = 2\pi(8)^2 \times 9.6 \times 10^{-3}/7$$

$$= 0.55 \text{ sq. mi. for 8 miles altitude}$$

$$\text{and } 55 \text{ sq. mi. for 80 miles altitude}$$

This corresponds to a 3° acceptance angle in both cases. By increasing the acceptance angle and, therefore, the lunar surface area viewed, signals above the minimum of $0.01\,\mu A$ can easily be obtained. However, for $0.01\,\mu A$ signal due to luminescence, the reflected background is at about $0.2\,\mu A$.

The best means of detecting the luminescence against the reflected background is by the Fraunhofer line technique. This involves comparing the shape of a solar Fraunhofer line to the same line in the lunar spectrum. It depends on the luminescence having a constant intensity over the line width of approximately 10 Å, an assumption that can be made if the luminescence is broad band, as has been the case in other studies as well as in this one. Let T_s and T_m represent for the sun and moon, respectively, the ratio of the intensity of the center of the line to the intensity of the continuum, and let I_f and I_c be the intensities of the center of the line and of the continuum, respectively, for the solar spectrum. Then, if there is no luminescence, the lunar radiation will be all reflected sunlight and

$$T_m = RI_f/RI_c = T_s$$

where R is the reflectance coefficient. Any luminescence L, will, however, be added equally over the width of the line and

$$T_m = (RI_f + L)/(RI_c + L)$$

$$= \frac{(RI_f/RI_c + (L/RI_c)}{1 + (L/RI_c)}$$

$$= (T_s + k)/(1 + k)$$

where $k = L/RI_c$ is the luminescence intensity expressed as a fraction of the lunar continuum. Solving for k,

$$k = (T_m - T_s)/(1 - T_m)$$

so that the luminescence intensity can be calculated from the solar and lunar Fraunhofer line intensities.

The solar spectrum from 2200 Å to 3300 Å is known to have a very dense array of Fraunhofer lines. Moreover, this method has been used successfully in ground-based observations of lunar luminescence in the visible wavelengths (Grainger, 1963). Grainger's instrument can detect as little as 2% luminescence; it is a grating instrument that uses a phototube detector, the

output of which is electronically compared with the output of a second phototube to eliminate background fluctuations. Such an instrument could be adapted to the lunar orbiting vehicle and, in a vacuum environment, might acquire additional stability and sensitivity. The narrow spectrum of a Fraunhofer line can be scanned rapidly enough to allow good data acquisition with the approximately 1-mile-per-second ground speed of the lunar orbiting vehicle. This technique requires a high resolution spectrograph. Such equipment is available or can be built. The technique also can be used with photographic recording of the spectrum, but errors in this method are too high, according to Grainger and Ring (1962). Differences in intensity that are due to lithologic variation would be apparent in the differences in measured k-values and are within the sensitivity range of the method.

The present study has not been able to establish with certainty that the ultraviolet-excited luminescence observed experimentally is devoid of narrow bands. If, with further study, narrow peaks could be shown to exist, such luminescence could be detected against the reflected background by comparing electronically the region of the peak with a neighboring region where the peak is absent. This could be done by dispersive techniques or with appropriate narrow band filter pairs, such as the interference filters which can now be made for any desired wavelengths. Even peaks, however, if sufficiently broad, will not disqualify the Fraunhofer line technique.

The above remarks also apply to the small luminescence excited by x-rays, protons, and electrons. Any luminescence on the sunlit side will have to be measured through a large reflected background.

The ultraviolet, and all other rectilinear radiation from the sun that reaches the moon, will fall off in incident intensity as the cosine of the angle of incidence. Thus, the energy reaching the lunar orbiting vehicle on the sunlit leg of the orbit will rise away from and fall toward the terminators. To some extent this may be compensated by the increase in luminescence due to falling surface temperature (see discussion of temperature, below) but this is probably small compared to the cosine decrease.

Detection of the ultraviolet luminescence signal on the dark side of the moon involves instrumentation capable of sensing of the order of 5×10^{-13} ergs/cm^2 sec. This flux in the 2000-3000 Å band corresponds to less than 1 or 2 photons/cm^2 sec which is, at best, on the fringe of present capability. Use of an ordinary spectrograph compounds the difficulty because, even with an f/2 instrument, $E_R \sim 0.03$ ED; for a 1 cm^2 slit area, D, $E_R \sim 2 \times 10^{-14}$.

Fortunately, the fact that the total luminescence intensity varies with composition makes it possible for mapping to be performed by allowing the phototube to look directly at the lunar surface and record the visible as well as the ultraviolet. The data of this study show that most of the luminescence is in the visible, which would increase the flux by at least an order of magnitude. In addition, efficiencies are higher; those calculated for protons show a factor of at least 20 and as much as 200 increase of the 5200 Å region over the 2000-3000 Å region. These alone account for some two to three orders of magnitude. Additional energy can be gathered by increasing the detector area and acceptance angle. A photocathode surface of 3 cm^2 and an acceptance

angle of 60°, for example, results in $E_R = 4.5\ E$, a factor of almost five. Cryogenic cooling of the photocathode to reduce thermal noise, and chopping techniques (in which the signal is interrupted at an AC rate and the AC signal is then amplified) to reduce what background exists, could improve this figure still more. Of course, viewing such a large area would necessarily reduce the mapping resolution.

The dark side flux, listed in table 9, is uncertain because most of the energy sources which reach the surface of the dark side of the moon are uncertain at present. The existence of a lunar magnetic field less than the minimum detectability of previous measurement is uncertain. The possibility that either solar wind particles or particles in the tail of the earth's magnetosphere do reach the lunar surface is, to some degree, dependent on the existence of this field. Solar cosmic rays are also a possible source during events. Galactic x-rays may contribute depending on the orientation of the surface in the galaxy. The possible existence of some of these less certain sources may well raise the incident energy to levels such that detectable luminescence could be excited.

Photoelectric vs Photographic Recording

The chief advantage of photographic recording is that it is a simple, reliable technique that produces high resolution data over the entire spectrum. Its chief disadvantages are that long exposure is required and that the plates must be developed before data can be studied or transmitted. The spectrum of the Isolite source, used for calibration in the proton experiments, was photographed with the Gaertner using the camera attachment. Twenty to thirty minutes were required to record a usable spectrum. Even if the lunar surface glowed as intensely as the Isolite, a twenty minute exposure would not be acceptable; in twenty minutes the orbiter passes over some 1200 miles. The requirement that the plates be developed before data can be retrieved prevents continuous monitoring of the response, which is of particular importance during the first exploratory missions. Even if photographic recording were feasible, one of two choices would have to be made. Many plates could be exposed in succession to give adequate areal coverage, but the data would not be available until much later, when the operator could develop and examine them. On the other hand, plates could be exposed, developed, and examined one at a time, but the number of exposures and, therefore, the amount of data obtained would be too small.

The photoelectric technique is both reliable and fast, and can provide continuous monitoring. The disadvantages of this technique are that scanning is required and that associated electronic equipment customarily used may be bulky and heavy. Scanning time could pose a problem if large regions of the spectrum are to be examined. The 2000-3000 Å region may be borderline in this regard, depending on how large an area of the lunar surface is viewed. However, to differentiate rocks on the basis of total intensity requires only part of the spectrum, to examine particular peaks, or pairs of peaks, for ratio purposes also requires only parts of the spectrum, and the Fraunhofer line technique requires only a narrow band of a few Ångstroms per line. Associated electronic equipment used for this technique need not be bulky and

heavy. In this study a small, relatively light-weight battery power supply was assembled and used with the EMI tube with excellent results. Ratio-taking electronics, chart recorders, and other associated equipment either exist in small, light-weight form, or can be so constructed with only moderate advances in design. Battery-powered photomultiplier tubes are recommended as the light detecting elements for the lunar orbiting vehicle.

Temperature Effects

Luminescence intensity generally increases with decrease in temperature (Kröger, 1948). Although the extent of this temperature effect in the rocks of this study is unknown, the result, so far as measurements from the lunar orbiting vehicle are concerned, is that any dark side luminescence would be enhanced at the same time that background due to solar electromagnetic radiation is absent. On the sunlit side, areas for which the sun is at the zenith would suffer the greatest luminescence degradation, but because of the temperature gradient away from the sub-solar point, degradation would decrease toward the terminators and poles. (The terminator area is interesting in that it is favorably located for increased luminescence intensity due to temperature and also for maximum polarization effects, as discussed in the section on polarization). Much remains to be learned about the temperature effect, especially whether the relations noted for the visible wavelengths also hold for the ultraviolet.

Effects of a Possible Lunar Atmosphere

The two chief effects of a lunar atmosphere on measurements of ultra-violet radiation from the moon would be (1) absorption of the signal from the solid surface, and (2) fluorescence of the atmosphere itself. The most recent upper limits for the density of the lunar atmosphere are 10^{-9} of the terrestrial sea level density based on optical methods, and 10^{-13} based on radio star occultation methods (Öpik, 1962; Bernstein, Fredricks, and Vogl, 1963). These refer to neutral particle densities, but the charged particle densities are estimated to be much lower by these authors. A vacuum so high will probably have negligible absorption or fluorescence effects, although Öpik states that certain spectral line emissions can be completely absorbed by the approximately 10^{13} atoms or molecules per cm^2 of lunar surface that would exist even with a density of 10^{-13} of the terrestrial.

Fluorescence of local, temporary atmospheres due to outgasing could well be observed if such a process takes place on the moon. Kozyrev's (1959) observation of a "volcanic eruption" in Alphonsus may have been a case of this kind although, according to Öpik (1962), this could not have been due to escaping gas because the emission was fixed in position and no spreading occurred. The color phenomena observed by Greenacre and Barr (Anonymous, 1964) in the vicinity of Aristarchus also appeared to be fixed in position. This lack of spreading could still be associated with gas eruption if it is assumed that a density gradient exists in the dispersing gas such that beyond the fluorescent area the gas is too tenuous for the fluorescence to be detected.

Color phenomena of the Aristarchus and Alphonsus variety could easily be seen by the astronaut in the lunar orbiting vehicle and, in fact, is probably more readily recognized by him than by an unmanned, instrumented vehicle. The maximum length of colored area in the Aristarchus observations was 12 miles; the Alphonsus "eruption" was approximately 4 miles in size. Thus, these areas are smaller than the total possible area that can be viewed from the lunar orbiting vehicle and should be distinguishable from the expected less intense, and more widespread, solid surface luminescence. It is not known whether any ultraviolet component was present in the observations, but the visible component, at least, was strong enough to allow Kozyrev to obtain a spectrum photographically. The proximity of the lunar orbiting vehicle to the lunar surface should allow spectra to be obtained either photographically or photoelectrically. If these phenomena are indeed due to gas eruptions, data on composition of the gases may be obtained.

If gas eruption and fluorescence occur on the moon, the luminescence of the solid surface beneath will be obscured or blotted out. If, however, the affected areas viewed from the lunar orbiting vehicle are the same size as those of the terrestrial observations, this should not cause many gaps in the mapping of the surface. Moreover, the time durations are such that an area affected during one orbit may be clear on the second or third orbit (approximately one-half hour and one hour duration for the two Aristarchus observations, respectively; between one-half and two and one-half hours for the Alphonsus observation).

Polarization Effects

Discrimination between lunar reflected light and luminescence may possibly be based on the fact that reflected light from the moon is partially polarized whereas the luminescence is expected to be isotropic. The polarization of the moon is greatest near first and third quarters, where it does not exceed 17%, and is zero at full moon, according to Bobrovnikoff's (1959) summary of the work of Lyot. If this same angular relationship holds for the orbiter, the maximum polarization would then be viewed near the terminators. Viewing through a polarizing filter could then possibly enhance the luminescence to background ratio because the polarized reflected light would be reduced by a greater proportion than the luminescence. If the polarization curve of the moon all along the path of the lunar orbiting vehicle were known, it might also be possible to detect luminescence in other areas besides those near the terminator. However, with a maximum polarization of less than 17%, the enhancement effect might not be great. Obviously, much more needs to be known about the polarization effect, especially as regards the degree to which the luminescence is polarized. It should also be noted that past polarization studies have had to do with visible light. Whether or not the same conclusions apply to ultraviolet light has yet to be determined.

Importance of the Astronaut

The presence of an astronaut, for at least the initial exploration observations, is preferable to an unmanned mission. Even if the luminescence

characteristics of terrestrial rocks were completely known, there would be no assurance that the lunar surface would conform to these known patterns. Radiation damage or sputtering, for example, are processes that might alter lunar surface characteristics even if the rocks, in their original state, were terrestrial counterparts. For this reason, the luminescence observations from the lunar orbiting vehicle should be performed by a man, who, unlike a machine, can exercise judgment, change plans as the situation requires, and take advantage of unforeseen phenomena and events. He can adjust and maintain the equipment, try various combinations of filters, slit adjustments, and other variables for best response, monitor and make at least preliminary analyses of the data, select important features of the landscape and of the data for more intensive observation, and select which data should be kept or returned to earth and which rejected. Once the lunar luminescence characteristics are known to the extent that measurements and data interpretation become routine, if this occurs, subsequent mapping missions could be accomplished by unmanned lunar orbiting vehicles.

RESUME OF RESULTS AND CONCLUSIONS

The reflectance and luminescence characteristics in the 2000-3000 Å range of granite, gabbro, and serpentinite samples, in solid and granular form, have been studied for the purpose of determining whether it is feasible to map the surface composition of the moon by spectral analysis in this range from a manned lunar orbiting vehicle at 8 to 80 miles altitude. Luminescence was excited by ultraviolet radiation, x-rays, protons, and electrons. Results of the experimental work are as follows:

(1) The reflectance curves for all samples are generally featureless. The reflectance declines gradually from 3000 Å to 2500 Å and still more gradually from 2500 Å to 2000 Å. No consistent variation with grain size was detected. Serpentinite shows, for the most part, a lower reflectance than granite and gabbro, which are approximately the same.

(2) In virtually all measurements, both of total luminescence and of luminescence spectra, the granite shows the greatest luminescence intensity, gabbro the next, and serpentinite the least. This is in harmony with luminescence data on minerals obtained in the Douglas Aircraft Company independent research studies in which the minerals of the acid igneous rocks show higher luminescence intensities than those of the basic igneous rocks.

(3) Decreasing grain size has, in general, the effect of reducing the luminescence intensity but this does not obscure the shape of the spectral curve. In some cases, however, intensity was observed to increase with decreasing grain size.

(4) Within the limits of the instrumentation used, luminescence spectra proved to be broad band, except as noted in (5), below. Features (other than intensity) of the spectral curves that reflected

compositional differences, such as peak positions, curve shapes, and so forth were observed chiefly in the wavelengths longer than 3000 Å. Similar features may be present in the 2000-3000 Å region but greater instrumentation sensitivity will be required to observe them.

(5) Sharp peaks at 3400 Å and 3600 Å, possibly due to line emission of an element or elements, were found with x-ray excitation in all samples. Additional peaks were found in serpentinite. These peaks appeared sharper and more of them occurred as the "continuum" luminescence intensity decreased because of either grain size or rock type differences. They also appeared to decline less in intensity than the continuum.

(6) In general, most of the luminescence occurred in the visible and near ultraviolet wavelengths; only a relatively small proportion was found in the 2000-3000 Å region.

(7) Measured efficiencies of luminescence in the 2000-3000 Å region were of the order of 1% for 1800-2200 Å ultraviolet excitation and of the order of 5×10^{-5}% and less for x-ray, proton, and electron excitation, within the limits of the instrumentation used. The ultraviolet and proton values are based on observed luminescence with these types of excitation; the x-ray and electron values are extreme upper limits because little or no 2000-3000 Å luminescence with these excitation types was observed in the spectral measurements.

These laboratory results were combined with available knowledge of the space radiation environment of the moon to determine the feasibility of compositional mapping under the conditions set forth for the study. The conclusions are as follows:

(1) On the sunlit side of the moon, luminescence energy in the 2000-3000 Å region is estimated to be high enough for detection; it must, however, be detected against a high reflected background. Virtually all of this luminescence is due to ultraviolet excitation.

(2) On the dark side of the moon little or no background of 2000-3000 Å light would be present, but the luminescence in this region would be due to x-rays, protons, and electrons and is estimated to be on the fringe of, or even beyond, present detection techniques if only the relatively certain sources of excitation are present. If, however, some uncertain sources of excitation are present, as, for example, particle radiation from the earth's magnetosphere, sufficient luminescence energy for detection may well exist.

(3) The detection problem is two-fold; on the sunlit side, a measurable signal must be detected against a high background, whereas on the dark side, a very small signal must be detected against essentially no background. For the sunlit side, it is considered feasible to measure the luminescence by the Fraunhofer line technique; that is, comparing the ratio of depth to continuum for a Fraunhofer line for

the sun and the moon. Photoelectric photometry is recommended for detection. Such instruments have already been successful in detecting lunar luminescence in the visible wavelengths from ground-based observatories.

(4) For the dark side, a sensitive phototube is recommended to view the surface directly, detecting visible as well as ultraviolet light and having as large an acceptance angle and photocathode surface area as is practicable.

(5) The compositional differences appearing in the experiments are of an order deemed detectable from the lunar orbiting vehicle. Relative intensity alone appears to provide a good basis for mapping compositional differences, and when tied in with laboratory luminescence tests on returned lunar rock samples from the first manned landings, it could also provide compositional determination.

RECOMMENDATIONS FOR FURTHER STUDY

Based on the results of this study, the following recommendations for further study are made:

(1) Continue the ultraviolet excitation studies in order to better define the luminescence spectra. In view of the high efficiencies for this energy source and the large amount of excitation energy available, ultraviolet-excited luminescence could be one of the most important sources of compositional information for large scale mapping of the lunar surface.

(2) Extend the studies to include the visible wavelengths. Much more luminescence occurs in these wavelengths than in the ultraviolet. This region is, therefore, especially important in mapping the dark side of the moon where luminescence intensity may be marginally detectable.

(3) Use selected minerals rather than rock samples. Rocks, being aggregates of minerals, have a wider range of composition and, hence, can be expected to show a less uniform response than minerals. With knowledge of the luminescence characteristics of the common rock-forming minerals, the characteristics of the rocks can easily be calculated.

(4) Continue the x-ray excitation studies to define and identify the possible line emission phenomena. This is the only appearance in this study of such peaks, and they deserve further study as a possible means of determining element composition.

(5) Initiate x-ray fluorescence studies of the same samples. X-ray fluorescence could give information on element composition and may be detectable at much lower flux levels than ultraviolet or visible luminescence.

REFERENCES

Allison, R.; Burns, J.; and Tuzzolino, A. J.: Absolute Fluorescent Quantum Efficiency of Sodium Salicylate. J. Opt. Soc. Am. vol. 54, 1964, pp. 747-751.

Anonymous: Lunar Color Phenomena, ACIC Technical Paper No. 12, U. S. Air Force, Aeronautical Chart and Information Center, 1964.

Baldwin, R. B.: The Measure of the Moon. University of Chicago Press, 1963, pp. 333-340.

Bernstein, W.; Fredricks, R. W.; and Vogl, J. L.: The Lunar Atmosphere and its Relationship to the Solar Wind. Proceedings of the Lunar and Planetary Exploration Colloquium, vol. 3, 1963, pp. 15-20.

Bobrovnikoff, N. T.: Natural Environment of the Moon. WADC Phase Technical Note 3, Wright Air Development Center, Ohio, 1959, pp. 77-81.

Bowyer, S.; Byram, E. T.; Chubb, T. A.; and Friedman, H.: Cosmic X-Ray Sources, Science, vol. 147, 1965, pp. 394-398.

Burns, E. A.: Instrumentation for a Mineralogical Satellite. XIVth International Astronautical Congress, Paris, 1963.

Cameron, A. G. W.: Particle Acceleration in Cislunar Space. Nature, vol. 202, 1964, p. 785.

Chapman, D. R.; and Larson, H. K.: On the Lunar Origin of Tektites. J. Geophys. Res., vol. 68, 1963, pp. 4305-4358.

Chubb, T. A.; Friedman, H.; and Kreplin, R. W.: X-Ray Emission Accompanying Solar Flares and Non-flare Sunspot Maximum Conditions. Space Research I, edited by H. K. Kallmann-Bijl, North-Holland Publishing Company (Amsterdam), 1960.

Compton, K.; and Allison, D.: X-Rays in Theory and Experiment. D. Van Nostrand Co., Inc., 1964, p. 90.

Friedman, H.: The Sun's Ionizing Radiations. Physics of the Upper Atmosphere, edited by J. A. Ratcliffe, Academic Press, 1960.

Grainger, J. F.: Lunar Luminescence Investigations, Astronomical Contributions from the University of Manchester. Series III, no. 104, University of Manchester, 1963.

Grainger, J. F.; and Ring, J.: The Luminescence of the Lunar Surface. Physics and Astronomy of the Moon, edited by Zdenek Kopal, Academic Press, 1962, pp. 397-399.

Hinteregger, H. E.: Solar Electromagnetic Radiation. Space and Planetary Environments, edited by Shea L. Valley, A. F. Cambridge Res. Labs., 1962.

Kopal, Z.; and Rackham, T. W.: Excitation of Lunar Luminescence by Solar Flares. Nature, vol. 201, 1964, pp. 239-241.

Kozyrev, N. A.: Observations of a Volcanic Process on the Moon. Sky and Telescope, vol. 18, 1959, p. 184.

Kreplin, R. W.: Solar X-Rays. Ann. Geophys., vol. 17, no. 2, 1961.

Kreplin, R. W.; Chubb, T. A.; and Friedman, H.: X-Ray and Lyman-Alpha Emission From the Sun as Measured From the NRL SR-1 Satellite, J. Geophys. Res., vol. 67, 1962, pp. 2231-2253.

Kröger, F. A.: Some Aspects of the Luminescence of Solids. Elsevier Publishing Company, 1948.

Masley, A. J.; and Goedeke, A. D.: Complete Dose Analysis of the November 12, 1960 Solar Cosmic Ray Event. Life Sciences and Space Research, edited by R. B. Livingston, A. A. Imshenetsky, and G. A. Derbyshire; North-Holland Publishing Company, (Amsterdam), 1963, pp. 95-109.

Middleton, W. E. K.; and Sanders, C. L.: The Absolute Spectral Diffuse Reflectance of Magnesium Oxide. J. Opt. Soc. Am., vol. 41, 1951, pp. 419-424.

Ness, N. F.: The Earth's Magnetic Tail. NASA Report X-612-64-392, Goddard Space Flight Center, 1964.

Ogilvie, K. W.; Bryant, D. A.; and Davis, L. R.: Rocket Observations of Solar Protons during the November 1960 Events, 1. J. Geophys. Res., vol. 67, 1962, pp. 929-937.

O'Keefe, J. A.; and Cameron, W. S.: Evidence From the Moon's Surface Features for the Production of Lunar Granites. Icarus, vol. 1, 1962, pp. 271-285.

Öpik, E. J.: The Lunar Atmosphere. Planetary Space Sci., vol. 9, 1962, pp. 211-244.

Salisbury, J. W.: The Origin of Lunar Domes. Astrophys. J., vol. 134, 1961, pp. 126-129.

Snyder, C. W.; and Neugebauer, M.: Interplanetary Solar Wind Measurements by Mariner II. Space Research IV, edited by P. Muller, North-Holland Publishing Company, (Amsterdam), 1964.

Spurr, J. E.: Geology Applied to Selenology. Rumford Press, 1945.

Sytinskaya, N. N.: New Data on the Meteor-Slag Theory of the Formation of the Outer Layer of the Lunar Surface. Soviet Astron. AJ, English Translation, vol. 3, 1959, pp. 310-314.

Urey, H. C.: The Planets. Yale University Press, 1952.

LIBRARY CARD ABSTRACT

The reflectance and luminescence characteristics in the 2000-3000 Å range of granite, gabbro, and serpentinite samples, in solid and granular form, have been studied for the purpose of determining whether it is feasible to map the surface composition of the moon by spectral analysis in this range from a manned lunar orbiting vehicle at 8 to 80 miles altitude. It was found that the rocks can be distinguished on the basis of luminescence intensity (granite highest, gabbro next, serpentinite lowest) and upon spectral curve shapes, peak positions, and other features, although most of these features are in wavelengths longer than 3000 Å. Luminescence efficiencies, combined with space radiation energy flux data, lead to the conclusion that such mapping is feasible on the sunlit side of the moon. On the dark side, however, luminescence is at or below present detectability limits unless, as is possible, more excitation energy is available than is estimated.